

Microscopic model of quantum butterfly effect: out-of-time-order correlators and traveling combustion waves

Igor L. Aleiner

Columbia Physics Department, 530 W 120th Street, New York, NY, 10027, USA

Lara Faoro and Lev B. Ioffe

*Laboratoire de Physique Theorique et Hautes Energies, CNRS UMR 7589
Universites Paris 6 et 7, place Jussieu 75252 Paris, Cedex 05 France*

*Department of Physics and Astronomy, Rutgers University, 136 Frelinghuysen Rd,
Piscataway 08854, New Jersey, USA*

Abstract

We extend the Keldysh technique to enable the computation of out-of-time order correlators such as $\langle O(t)\tilde{O}(0)O(t)\tilde{O}(0)\rangle$. We show that the behavior of these correlators is described by equations that display initially an exponential instability which is followed by a linear propagation of the decoherence between two initially identical copies of the quantum many body systems with interactions. At large times the decoherence propagation (quantum butterfly effect) is described by a diffusion equation with non-linear dissipation known in the theory of combustion waves. The solution of this equation is a propagating non-linear wave moving with constant velocity despite the diffusive character of the underlying dynamics.

Our general conclusions are illustrated by the detailed computations for the specific models describing the electrons interacting with bosonic degrees of freedom (phonons, two-level-systems etc.) or with each other.

Keywords: Quantum butterfly, decoherence, out-of-time-order.

Contents

1	Motivation	2
2	Augmented Keldysh and Keldysh techniques	4
2.1	Augmented Keldysh technique	4
2.2	Augmented space and Green function	6
2.3	Observables and computables	8
2.4	Dyson equation.	9

2.5	Stability and instability.	10
2.6	Basic rules of the diagram technique: Green functions	12
2.7	Vertices	13
2.8	Diagram technique: summary	15
3	Microscopic Models	16
3.1	Electron-phonon interaction	17
3.2	Electrons in disorder potential	18
3.3	Electron-electron interaction	19
4	Kinetic equation for normal and augmented Keldysh functions.	19
4.1	Quasiclassical descriptions	19
4.2	Collision integrals for the specific models	20
4.2.1	Electron-phonon scattering.	21
4.2.2	Electron-electron scattering.	22
4.3	Electron-impurity scattering	24
4.4	Additional remarks	24
5	Instability of the augmented Keldysh functions in zero dimensional case	25
5.1	Instability in electron-phonon model.	25
5.1.1	Classical limit ($\omega_0 \ll T$)	26
5.1.2	Quantum limit ($\omega_0 \gg T$)	27
5.2	Instability for electron-electron interaction.	29
6	Equations for spatial structure of the instability	30
7	Spatial Propagation of the instability: combustion waves.	31
8	Time and spatial dependence of out-of-time-ordered correlators.	33
9	Discussion and conclusions	36
10	Acknowledgement	37

1. Motivation

In a chaotic classical system a small perturbation leads to the exponential divergence of trajectories characterized by Lyapunov time, $1/\Lambda$. As a result, the observables in two copies of the system experiencing different perturbations quickly become uncorrelated. In a many body system a *local* perturbation initially destroys the correlations locally, then the region where the correlations are destroyed quickly grows with time. Killing a butterfly in Ray Bradbury story [1] leads to the spreading perturbation until it reaches the size of the system (Earth in this story). This phenomena is known as butterfly effect.

The concept of butterfly effect can be generalized to a closed chaotic quantum system even though such generic system does not necessarily have a direct analogue of Lyapunov divergence of trajectories because quantum mechanics prohibits the infinitesimal shift of the trajectory. The convenient measure of the butterfly effect is provided by the out-of-time-order correlator (OTOC) that was first introduced by Larkin and Ovchinnikov[2], revived by Kitaev [3, 4] and extensively discussed by a number of works recently [5, 6, 7, 8]. OTOC is defined by

$$\mathcal{A}(t) = \left\langle O(t)\tilde{O}(0)O(t)\tilde{O}(0) \right\rangle, \quad (1)$$

where $O(t)$ and $\tilde{O}(t)$ are two local operators in Heisenberg picture. Physically, it describes how much the perturbation introduced by $\tilde{O}(0)$ changes the value of the $O(t)$. At large times $\mathcal{A}(t)$ goes to a zero, because the state created by the consecutive action of the operators $O(t)\tilde{O}(0)$ is incoherent with the state obtained when these operators act in a different order.¹ The anomalous time order in the correlator (1) implies the evolution backward in time, so it is not measurable by direct physical experiments on one copy of the system in the absence of a time machine such as implemented in NMR experiments [9]. One can view the decrease of the OTOC with time as the consequence of the dephasing between two initially almost identical Worlds evolving with the same Hamiltonian. In this respect it is different from the problems of fidelity [10] and Loschmidt echo ([9] and references therein) that study evolution forward and backwards with slightly different Hamiltonians. It is also different from a problem of the evolution of a particle along quasiclassically close trajectories appearing in studies of the proximity effects [2] or weak-localization [11] and quantum noise [12].

For physical systems the Hamiltonian is local, so that distant parts of a system are not interacting directly with each other. In this case, one may further distinguish the case when operators O and \tilde{O} act far from each other in real space. One expects that the correlator decreases after the significant delay needed for the perturbation to spread over the distance separating these operators. When correlators of this type decayed for *any* separation between the operators in the real space the coherence is completely lost. The decay of OTOC at long times for all subsystems (i.e. for all separations) for all operators O and \tilde{O} implies complete quantum information scrambling [13]. Note that the separation of the operators in space is equivalent to the separation into subsystems introduced in quantum information works. We are not going to discuss here quantum information implications of OTOC and the exact definition of quantum scrambling; we refer the reader to the literature that discussed its theory [14, 15, 16, 17, 18] and the possibility of its experimental measurement [19, 20].

The goal of this work is to develop the analytic tools to study OTOC (1) for microscopic models that allow for the solutions for conventional correlators.

¹Here we assume that operators O have zero averages in all states. If not, the irreducible correlators have to be discussed. We also assume that operator $\langle O^2(t) \rangle \neq 0$

The technique that we develop is essentially a straightforward extension of the Keldysh technique. We apply our technique to three models that are basic in condensed matter physics: (i) electrons interacting with localized bosonic degrees of freedom (Einstein phonons or simplified two level systems), (ii) electrons in the disorder potential and (iii) electrons weakly interacting with each other. We find that in models (i) and (iii) the mathematical description of the OTOC is similar to the description of the combustion waves. The small initial perturbation first grows exponentially remaining local and then starts to propagate with a constant velocity and a well defined front, despite the fact that the thermal transport in these models is always diffusive. The velocity of the front propagation is always slower than electron Fermi velocity and it is parametrically slower than it in some models. The apparently slow velocity of the front propagation implies that it does not necessarily saturate Lieb-Robinson bound [21]. This conclusion of the constant velocity of the quantum butterfly propagation agrees with the result obtained in holographical theory of black holes [6, 22, 23].

The plan of this paper is the following. In Section 2 we introduce the basic elements of our technique: the augmented Keldysh formalism that involves two forward and two backward paths. The state of the system in this formalism is described by the diagonal and off-diagonal Green functions in the augmented space. The diagonal functions describe the quasiparticle distribution function in each “world”, the off-diagonal ones describe the coherence between the “worlds”. In Section 2.3 we introduce two types of correlators that one can compute in this technique: the observables that can be measured directly in a physical experiment and the computables that one can only compute numerically (or measure given the time machine). In Section 3 we introduce the details of the microscopic models for which the anomalous correlator of type (1) will be computed. In Section 4 we derive the analogue of the kinetic equation for both diagonal and off-diagonal ones. In Section 5 we analyze the stability of the kinetic equations of Section 4 ignoring their spatial structure (i.e. in zero dimensional case) and show that the instability of the off-diagonal functions is described by non-linear ordinary differential equations. Section 6 generalizes these equations for the models with spatial structure for which they become similar to the equations describing the combustion waves. Section 7 describes the formation of the propagating front that follows from the non-linear diffusive equations derived in Section 6. The Section 8 studies the initial time period at which the state of the system is not yet accounted for by the diffusive equations and its match to the evolution at longer times. Finally, the Section 9 gives the summary of the results and discussions of possible extensions.

2. Augmented Keldysh and Keldysh techniques

2.1. Augmented Keldysh technique

Anomalous ordered correlator such as out of time ordered $\mathcal{A}(t)$ introduced in the Section 1, see Eq. (1), cannot be computed in conventional techniques that assumes casual time evolution. To circumvent this difficulty we augment

the standard Keldysh technique by introducing two forward and two backward evolutions shown in Fig. 1b.

In order to describe the augmented technique we recall the conventional Keldysh technique [24] first. There, the differently ordered correlators are given by

$$N_{\alpha\beta\gamma\delta}(t) = \left\langle \mathcal{T}_{C_K} \hat{O}_\alpha(t_2) \hat{O}_\beta(t_1) \hat{O}_\gamma(t_2) \hat{O}_\delta(t_1) \exp \left(-i \int_{C_K} \hat{H}_{int}(t) dt \right) \right\rangle, \quad (2)$$

where $\alpha, \beta, \gamma, \delta = \pm$ denote the positions of the operators on the traditional Keldysh contour shown in Fig. 1a. Here all observable operators \hat{O} and the interaction part of the Hamiltonian \hat{H}_{int} are in the interaction representation, the averaging is done with a density matrix (that represents the initial conditions in the past), the symbol \mathcal{T}_{C_K} denotes ordering of the operators on the Keldysh contour, i.e. the operator referring to the position down the contour is on the left in (2) (for fermion operators the change of order brings in minus sign). One can see that by choosing indexes $\alpha, \beta, \gamma, \delta = \pm$ one can get different order of operators but never the anomalous order required by Eq. (1).

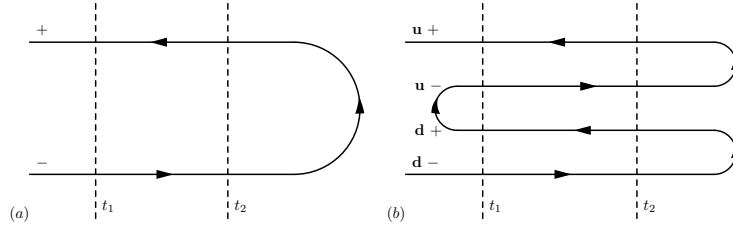


Figure 1: The traditional, C_K , (a) and the augmented (b) Keldysh contours C_{aK} . Times $t_{1,2}$ label the insertion of the operators for observable or computable quantities, see text. Operators (fermionic or bosonic) are ordered according their location on the contours C_K , C_{aK} .

The augmented contour C_{aK} allows anomalous order of the operators such as in Eq. (1). For this contour the indices $\alpha, \beta, \gamma, \delta$ can acquire four values, $u\pm, d\pm$ (where u stays for the up and d for the down parts of the contour). The expression similar to Eq. (2)

$$A_{\alpha\beta\gamma\delta}(t) = \left\langle \mathcal{T}_{C_{aK}} \hat{O}_\alpha(t_2) \hat{O}_\beta(t_1) \hat{O}_\gamma(t_2) \hat{O}_\delta(t_1) \exp \left(-i \int_{C_{aK}} \hat{H}_{int}(t) dt \right) \right\rangle, \quad (3)$$

with the choice $\alpha = u+, \beta = d+, \gamma = u-, \delta = d-$ becomes out-of-order correlator $\mathcal{A}(t)$. Clearly other combinations of indices will produce normal as well abnormal correlators.

Equation (3) is the essence of the augmented technique. Unitary evolution on u/d segments of the contour can be viewed as the evolution of the different worlds (we will use this term loosely throughout the paper) with the same Hamiltonian and the same initial conditions (“correlated worlds “ initially). The correlator (3) can be viewed as the response at time t to the perturbation (source) at time

0. When the sources are located at the same up/down parts of the contour, the response is directly measurable, we shall refer to these sources as 'physical'. All the other sources will be referred to as 'unphysical'. Our ultimate objective is to describe how these "correlated worlds" become "uncorrelated worlds" provided that a small local perturbation is seeded differently in the two worlds (butterfly effect).²

In the next few sections we generalize the rules and the results of Keldysh technique for the augmented Keldysh technique. We will see that almost all rules are going through up to the kinetic equation where the correlation function describing not only the occupation numbers but also the measure of the correlation between the different worlds.

2.2. Augmented space and Green function

Similarly to usual diagrammatic technique, we introduce the 4×4 matrix of Green functions of Fermi or Bose fields. It is convenient to view this four dimensional space as a direct product of 2×2 Keldysh and 2×2 augmented space. Each operator (fermionic or bosonic) $\psi(t)$ can be placed in four different points of contour at time t , therefore it is enlarged into four dimensional vector:

$$\Psi(1) = \begin{bmatrix} \psi_u(1) \\ \psi_d(1) \end{bmatrix}_a; \quad \psi_i(1) = \begin{bmatrix} \psi_{i,+}(1) \\ \psi_{i,-}(1) \end{bmatrix}_K \quad (4)$$

where (1), (2) are the short hand notations for the coordinates, times (and might be spin) that specifies the single particle state: $i \equiv (t_i, r_i, \sigma_i)$. In these notations the 4×4 matrix Green function reads

$$i\hat{\mathcal{G}}(1, 2) = \langle \mathcal{T}_C \Psi(1) \otimes \Psi^\dagger(2) \rangle. \quad (5)$$

As usual, the components of the Green functions are linearly dependent. This redundancy is eliminated by the Keldysh rotation, which is conveniently described by the Pauli matrices

$$\begin{aligned} \hat{\tau}_0 &= \begin{pmatrix} 1 & 0 \\ 0 & 1 \end{pmatrix}; \quad \hat{\tau}_1 = \begin{pmatrix} 0 & 1 \\ 1 & 0 \end{pmatrix}; \quad \hat{\tau}_2 = \begin{pmatrix} 0 & -i \\ i & 0 \end{pmatrix}; \quad \hat{\tau}_3 = \begin{pmatrix} 1 & 0 \\ 0 & -1 \end{pmatrix}; \\ \hat{\tau}_+ &= \begin{pmatrix} 0 & 1 \\ 0 & 0 \end{pmatrix}; \quad \hat{\tau}_- = \begin{pmatrix} 0 & 0 \\ 1 & 0 \end{pmatrix}. \end{aligned} \quad (6)$$

The superscript, $\cdot = a, K$, describes the space (augmented or Keldysh) in which these matrices act. In terms of matrices (6) the Keldysh rotation is given by³

²The two contour formalism of Ref. [25] is not suitable for this purpose: in this formalism the worlds are uncorrelated from the very beginning though the disordered potential acts the same on the both worlds.

³Such parametrization of the Keldysh space was first introduced by Larkin and Ovchinnikov [26].

$$\Psi \rightarrow \hat{\mathcal{R}}\Psi, \quad (7a)$$

$$\Psi^\dagger \rightarrow \bar{\Psi} = \Psi^\dagger \hat{\mathcal{R}}^\dagger \cdot (\hat{\tau}_1^K \otimes \hat{\tau}_0^a), \quad (7b)$$

$$\hat{\mathcal{G}} \rightarrow (\hat{\mathcal{R}}\hat{\mathcal{G}}\hat{\mathcal{R}}^\dagger) \cdot (\hat{\tau}_1^K \otimes \hat{\tau}_0^a), \quad (7c)$$

$$\hat{\mathcal{R}} = \exp\left(\frac{i\pi\hat{\tau}_2^K \otimes \hat{\tau}_0^a}{4}\right) \quad (7d)$$

After rotation (7), the Green function acquires the form

$$\hat{\mathcal{G}} = \begin{pmatrix} \hat{G}_{uu} & \hat{G}_{ud} \\ \hat{G}_{du} & \hat{G}_{dd} \end{pmatrix}_a,$$

where

$$\begin{aligned} \hat{G}_{uu} &= \begin{pmatrix} G^R & G^K \\ 0 & G^A \end{pmatrix}_K, \quad \hat{G}_{ud} = \begin{pmatrix} 0 & \Gamma^K \\ 0 & 0 \end{pmatrix}_K \\ \hat{G}_{du} &= \begin{pmatrix} 0 & \bar{\Gamma}^K \\ 0 & 0 \end{pmatrix}_K, \quad \hat{G}_{dd} = \begin{pmatrix} \tilde{G}^R & \tilde{G}^K \\ 0 & \tilde{G}^A \end{pmatrix}_K. \end{aligned} \quad (8)$$

In the absence of the non-physical sources⁴, the components diagonal in the augmented space are equal, $\hat{G}_{uu} = \hat{G}_{dd}$, and coincide with the conventional Green functions. In particular, the retarded, advanced and Keldysh Green functions, $G^{R,A,K}$ are given by

$$\begin{aligned} iG^R(1,2) &= \langle \psi(1)\psi^\dagger(2) \pm \psi^\dagger(2)\psi(1) \rangle \theta(t_1 - t_2), \\ iG^A(1,2) &= -\langle \psi(1)\psi^\dagger(2) \pm \psi^\dagger(2)\psi(1) \rangle \theta(t_2 - t_1), \\ iG^K(1,2) &= \langle \psi(1)\psi^\dagger(2) \mp \psi^\dagger(2)\psi(1) \rangle, \end{aligned} \quad (9)$$

(hereinafter, the upper sign corresponds to fermions and lower to bosons unless stated otherwise), whilst the inter-world functions read:

$$\begin{aligned} \Gamma^K(1,2) &= -2i \langle \psi(1)\psi^\dagger(2) \rangle = G^K(1,2) + [G^R(1,2) - G^A(1,2)], \\ \bar{\Gamma}^K(1,2) &= \pm 2i \langle \psi^\dagger(2)\psi(1) \rangle = G^K(1,2) - [G^R(1,2) - G^A(1,2)]. \end{aligned} \quad (10)$$

In the absence of non-physical sources, these functions include the information on the single particle spectrum and on the distribution functions of holes (particles), Γ^K ($\bar{\Gamma}^K$). We note that even in the presence of non-physical sources the diagonal components are not influenced by the non-diagonal ones. This is because the correlations between the upper and down worlds can not affect the dynamics in each of these worlds. Formally, this means that the structure of the Green functions always retain the form of Eq.(8). Only the relation (10) between diagonal and non-diagonal components in augmented space can be modified by the presence of non-physical sources. In fact, the violation of the relation (10) will be the formal indicator of the quantum butterfly effect.

⁴We distinguish physical sources that can be realized in experiment and the non-physical ones that require time-machine for their implementation

2.3. Observables and computables

We distinguish the correlators (*observables*) that can be in principle measured by a physics experiment and the ones that can only be studied in the rather artificial system that allows inversion of time directions. Because the latter can be more readily studied by numerical simulations, where the unitary evolution can be formally reversed⁵, we call them *computables*.

The example of observable is given by the casual correlator

$$\mathcal{N}_{\rho\rho}(t) = \frac{1}{2} \langle T_{\mathcal{C}} (\bar{\Psi}(t)(\tau_1^K \otimes \tau_0^a) \Psi(t)) (\bar{\Psi}(0)(\tau_0^K \otimes \tau_0^a) \Psi(0)) \rangle \quad (11)$$

that describes the density response at time t to the perturbation at time 0. Indeed the correlator (11) rewritten in terms of the original fields ψ has the form

$$\mathcal{N}_{\rho\rho}(t) = \langle [\psi^\dagger(t, r) \psi(t, r), \psi^\dagger(0, r_0) \psi(0, r_0)] \rangle,$$

the usual rules of linear response imply that the density induced by the scalar potential applies at point r_0 at time $t = 0$ is given by $-i\mathcal{N}_{\rho\rho}(t)$. In fact this structure is general for Keldysh technique: the physical perturbation comes with τ_0^K while the observable comes with τ_1^K .

In contrast the out-of-time-ordered correlator provides the example of the computable. In this paper we focus on out-of-time-ordered correlators of the form

$$\mathcal{A}_{\alpha\beta}^{\gamma\delta}(t, r; t' r') = \left\langle T_{\mathcal{C}} \left(\psi_\alpha(t, r) \psi_\beta^\dagger(t', r) \right) (\psi_\gamma^\dagger(0, 0) \psi_\delta(0, 0)) \right\rangle \quad (12)$$

that becomes out-of-time-ordered for many combinations of indices $\alpha, \beta, \gamma, \delta$. For instance, for $\alpha = u+, \beta = d+, \gamma = u-, \delta = d-$ it provides an example of the general correlator (3) discussed in Section 2.1. It is convenient to separate, as we have done here by parenthesis, the 'source' term provided by the product of two operators at time $t = 0$ and the 'response term' provided by two operators at time $t \approx t' > 0$.

For the fixed γ and δ the correlator (12) can be viewed as the Green function $G_{\alpha\beta}(t, r; t', r)$ computed in the states modified by the action of the operators $\psi_\gamma(0, 0) \psi_\delta^\dagger(0, 0)$. In particular, it satisfies the same identities as the Green function:

$$\mathcal{A}_{u+, d-}^{\gamma\delta} = \mathcal{A}_{u-, d-}^{\gamma\delta} = \mathcal{A}_{u-, d+}^{\gamma\delta} = \mathcal{A}_{u+, d+}^{\gamma\delta}. \quad (13)$$

After Keldysh rotation in indices α and β the correlator (12) acquires the same general form as the Green function (8).

Because of the identities (13) one can choose many equivalent forms of the out-of-time-ordered correlators that display unusual behavior. It will be more convenient to us to compute the symmetrized correlator defined by

$$\mathcal{A}_{\rho\rho}(t, t', r) = \left\langle T_{\mathcal{C}} (\bar{\Psi}(t', r)(\tau_1^K \otimes \tau_1^a) \Psi(t, r)) \hat{\mathcal{S}}_0 \right\rangle. \quad (14)$$

⁵Butterfly effect in this case might appear due to the rounding errors in back and forth evolutions.

The source term, $\hat{\mathcal{S}}_0$, can have many equivalent forms that distinguish upper and down Worlds, we can choose for instance

$$\hat{\mathcal{S}}_0 = \psi_{u-}^\dagger(0,0)\psi_{d-}(0,0) \quad (15)$$

This term destroys one particle in the down World and creates it back before the evolution in the upper World starts (notice that for the operators at $t = 0$ $\psi_{u-}^\dagger(0) = \psi_{d+}^\dagger(0)$, see Fig. 1). As we shall see below the final results depend very weakly on the particular form of the source term.

The response operator in this correlator is the sum of four terms

$$\hat{\mathcal{R}}_{tt'}(r) = \bar{\Psi}(t', r)(\tau_1^K \otimes \tau_1^a)\Psi(t', r) = \psi_{u-}^\dagger\psi_{d-} - \psi_{u-}\psi_{d-}^\dagger + \psi_{u+}^\dagger\psi_{d+} - \psi_{u+}\psi_{d+}^\dagger \quad (16)$$

that measures the product of the distribution functions and the correlations between the worlds. The minus sign in this equation is due to fermionic commutation rules.

As usual, any correlator allows for a pictorial representation to facilitate the basic structure of the theory and to be able to sum up the most important parts of the perturbative expansions up to infinite order. We develop the diagrammatic rules for the technique in the augmented space below in sections 2.6, 2.7, 2.8.

In the absence of the unphysical sources the two worlds remain perfectly correlated. The stability of this solution can be discussed in very general terms without the knowledge of the details of the microscopic model. In fact, the existence of the self-energy, Dyson equation, and the general thermodynamic relations are sufficient to prove that the perfectly correlated solution is unstable. We begin with these general considerations.

2.4. Dyson equation.

In any field theory that allows the separation of the Hamiltonian into bare (H_0) and interacting (H_{int}) parts, one can introduce the notion of bare Green function, \hat{G}_0 , corresponding to Hamiltonian H_0 , the full Green functions (defined above) and the self energies, $\hat{\Sigma}$, that take into account the effects of the interaction on the bare Green functions. In diagramm technique the self-energy can be defined as the sum of all one-particle-irreducible diagrams (see Sections 2.6, 2.7, 2.8). The Green functions and self-energies obey the Dyson equation that can be written in two equivalent forms

$$(\hat{H}_0\tau_0^a - \hat{\Sigma}) \circ \hat{G} = \hat{1}, \quad (17a)$$

$$\hat{G} \circ (\hat{H}_0\tau_0^a - \hat{\Sigma}) = \hat{1}, \quad (17b)$$

where $\hat{1}$ is the unit operator in the space-time and the augmented Keldysh space, the symbol \circ implies the matrix multiplication in the augmented space and the convolution in space-time. The operator \hat{H}_0 is diagonal in Keldysh and augmented spaces with the diagonal elements defined by equations $\hat{H}_0 G_0^R = 1$, $\hat{H}_0 G_0^A = 1$, it is related to the Hamiltonian H_0 by $\hat{H}_0 = id/dt - H_0$.

The general structure of the Green functions (8) implies that the parts of the Green function that are retarded and advanced in Keldysh space remain diagonal in the augmented space. Because the bare retarded and advanced Green functions are diagonal in the augmented space, the self energies $\Sigma_{\alpha\beta}^{A,R} = \delta_{\alpha\beta}\Sigma_{\alpha}^{A,R}$ remain also diagonal and they are given by the solution of the equations

$$(\hat{H}_0 - \Sigma_{\alpha}^{R/A}) \circ G_{\alpha}^{R/A} = 1 \quad (18a)$$

$$G_{\alpha}^{R/A} \circ (\hat{H}_0 - \Sigma_{\alpha}^{R/A}) = 1, \quad \alpha = u, d. \quad (18b)$$

As usual, the non-diagonal part of the Green functions in Keldysh space is not entirely determined by the Eqs. (18): it also depends on the initial conditions. Its evolution is described by the homogeneous equations

$$(\hat{H}_0 - \Sigma_{\alpha}^R) \circ G_{\alpha\beta}^K - \Sigma_{\alpha\beta}^K \circ G_{\beta}^A = 0, \quad (19a)$$

$$G_{\alpha\beta}^K \circ (\hat{H}_0 - \Sigma_{\beta}^A) - G_{\alpha}^R \circ \Sigma_{\alpha\beta}^K = 0. \quad (19b)$$

Notice that both the diagonal and the non-diagonal parts $G_{\alpha\beta}^K$ are controlled by the initial conditions. We emphasize that the diagonal components $\Sigma_{\alpha}^{A,R}$, $\Sigma_{\alpha\alpha}^K$ may depend on the diagonal components of the Green functions in the augmented space, $G_{\alpha\alpha}^K$, but not on the other diagonal (e.g. $G_{\beta}^{A,R}$, $G_{\beta\beta}^K$, $\beta \neq \alpha$) or the non-diagonal ($G_{\alpha\beta}^K$) Keldysh components. This observation turns out to be the key of the description of the instability in the evolution of non-diagonal correlations as we see in the next subsection.

2.5. Stability and instability.

Let us consider the fermionic Green function for the sake of concreteness. The Keldysh components of the Green function can be conveniently parametrized via

$$G_{\alpha\beta}^K = G_{\alpha}^R \circ \mathcal{F}_{\alpha\beta} - \mathcal{F}_{\alpha\beta} \circ G_{\beta}^A. \quad (20)$$

For $\alpha = \beta$ this equation reduces to the conventional parametrization of G^K in terms of the quantum distribution function, \mathcal{F}_{uu} and \mathcal{F}_{dd} ; for $\alpha \neq \beta$ it gives the parametrization of the new functions Γ^K and $\bar{\Gamma}^K$ in terms of \mathcal{F}_{ud} and \mathcal{F}_{du} .

Substituting Eq.(20) into Eqs. (19) and using Eqs. (18), we find that Eqs. (19) are satisfied for $\mathcal{F}_{\alpha\beta}$ solving the quantum kinetic equation

$$H_0 \circ \mathcal{F}_{\alpha\beta} - \mathcal{F}_{\alpha\beta} \circ H_0 = [\Sigma_{\alpha}^R \circ \mathcal{F}_{\alpha\beta} - \mathcal{F}_{\alpha\beta} \circ \Sigma_{\alpha}^A] - \Sigma_{\alpha\beta}^K. \quad (21)$$

In the quasiclassical approximation the two terms in brackets correspond to the outgoing scattering processes (this term taken alone always leads to dissipation) whilst the last term corresponds to the incoming processes (this term taken alone always leads to instability).

In thermal equilibrium the Green functions depend only on the time difference. The diagonal parts of the electron self energies are related by the fluctuation-dissipation theorem (FDT):

$$\Sigma_{\alpha\alpha}^K(\epsilon) = [\Sigma_{\alpha}^R(\epsilon) - \Sigma_{\alpha}^A(\epsilon)] n_0(\epsilon), \quad n_0(\epsilon) = \tanh\left(\frac{\epsilon - \mu}{2T}\right) \quad (22)$$

where ϵ is the frequency conjugated to the time difference, μ is the chemical potential, and T is the temperature: both of them are determined by the initial conditions. For Bosons one should replace $n_0(\epsilon) = \tanh(\dots)$ by $p_0(\omega) = \coth(\dots)$. For phonons (which number is not conserved) the chemical potential $\mu = 0$. In equilibrium the left hand side of Eq. (21) is zero, substituting Eq. (22) into (21) we see that $[1 - \mathcal{F}_{uu}(\epsilon)]/2$ has the meaning of the Fermi distribution function. The FDT also implies that Eq. (21) has a generally stable solution. The only reason for this solution to become unstable is the metastability of the state that might happen on the unstable branch of the phase transition. However, even in this case, the ultimate fate of the system is a different equilibrium characterized by different $\Sigma_{\alpha}^{R,A}$ and

$$\mathcal{F}_{uu} = \mathcal{F}_{dd} = n_0(\epsilon), \quad (23)$$

with different μ and T that are found from the number of particle and energy conservation in the new spectrum. That solution would be stable again.

The stability of the thermal solution of Eq. (21) is guaranteed by Boltzmann H -theorem and the global conservation laws (energy and the number of particles). In the framework of Eq. (21) it means that for small deviations of \mathcal{F}_{uu} , \mathcal{F}_{dd} from the thermal distributions the outgoing terms dominate incoming ones in Eq. (21). This fact is far from trivial because both terms are generically non-linear.

The equation (21) allows for solution similar to Eq. (23) for the off-diagonal components:

$$\mathcal{F}_{ud} = 1 + n_0, \quad \mathcal{F}_{du} = -1 + n_0. \quad (24)$$

We will call this solution the ‘‘correlated worlds solution’’.

In the Pauli matrix notation given by Eq. (6), Eq. (23) and Eq. (24) can be compactified (for fermions) as

$$\hat{\mathcal{F}} = n(\epsilon, p, r, t) (\hat{\tau}_0^a + \hat{\tau}_1^a) + i\hat{\tau}_2^a, \quad (25)$$

where anticipating further applications, we allow the distribution function to depend not only on energy but also on the phase space variable and time. The precise definition of the notion of the semiclassical phase space is given in Sec. 4.

Notice that in contrast to the solution Eq. (21), the stability of the correlated worlds solution is not guaranteed even if the solution Eq. (23) is stable. Indeed, for the diagonal (conventional) distribution function the small deviation from equilibrium results in the non-zero RHS of Eq. (21) in which outgoing terms always dominate incoming ones. Outgoing terms always imply relaxation, which

leads to the stability of the equilibrium solution. For non-diagonal distribution function, the small deviation from equilibrium results in the same incoming terms as for diagonal distribution function but smaller outgoing terms. A small deviation of diagonal term leads to two contributions to the outgoing term: one due to the interaction induced change in $\Sigma_\alpha^{A,R}$, another due to the change in \mathcal{F}_{uu} (\mathcal{F}_{dd}) itself. Because $\Sigma_\alpha^{A,R}$ do not depend on the off-diagonal terms \mathcal{F}_{ud} (\mathcal{F}_{du}), the former contribution is missing for the off-diagonal terms. This makes deviation of the outgoing term that tries to restore equilibrium smaller for non-diagonal distribution function in the interacting system. Thus, for the off-diagonal distribution function the outgoing terms do not necessarily dominate the incoming ones for small deviations from the equilibrium. This results in a possible instability of the solution of Eqs. (24). The computations for the specific models below show that this instability is indeed present for electron-phonon and electron-electron interactions but not for impurity scattering.

The alternative solution (allowed by conservation laws for off-diagonal components) is

$$\mathcal{F}_{ud} = \mathcal{F}_{du} = 0, \text{ or } \hat{\mathcal{F}} = n(\epsilon, p, r, t) \hat{\tau}_0^a, \quad (26)$$

this solution will be called the “uncorrelated worlds solution”.

The incoming term is second order (or higher) in \mathcal{F}_{ud} (\mathcal{F}_{du}), therefore it vanishes for the small deviation from this solution. In contrast, the outgoing term is always linear in \mathcal{F}_{ud} (\mathcal{F}_{du}) and it dominates. Thus, the uncorrelated worlds solution is generally stable and one expects that the correlated worlds solution (24) is not. The only exception is the electron scattering by impurities that conserves the number of particles at each energy separately. In this case both outgoing and incoming terms are linear in all components of $\mathcal{F}_{\alpha\beta}$ and the previous arguments do not hold.

The meaning of the “uncorrelated worlds solution” (26) is the following. Unlike their diagonal counterparts, \mathcal{F}_{ud} (\mathcal{F}_{du}) encode not only the distribution functions but also the overlap of the many-body wave-functions evolving at the upper and lower contour. Any decrease of this correlation diminishes the values of both \mathcal{F}_{ud} (\mathcal{F}_{du}). The proposed instability is therefore nothing but the quantum butterfly effect, the decay of \mathcal{F}_{ud} (\mathcal{F}_{du}) everywhere in the system results in the loss of the coherence between many body wave functions describing upper and down Worlds. The ultimate solution given in Eq. (26) corresponds to the complete destruction of the coherence between lower and upper contour.

The description of the evolution of the system from the “correlated worlds solution” (25) to the “uncorrelated worlds solution” (26) is the subject of the further sections.

2.6. Basic rules of the diagram technique: Green functions

The basic elements of the diagrammatic representation needed to compute the correlators in the augmented space are shown in Fig. 2. Notice that for keeping track of the Keldysh structure putting arrows on the Green function for the real fields (as it is done throughout this paper) is convenient but not

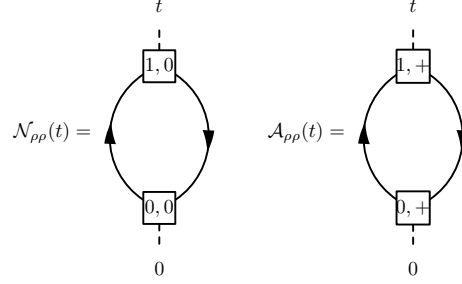


Figure 3: Diagrammatic expressions for the correlators (11) and (14) in non-interacting problem.

where

$$\begin{aligned}\gamma_{ij}^1 &= \tilde{\gamma}_{ij}^2 = \frac{1}{\sqrt{2}} [\hat{\tau}_0^K]_{ij}, \\ \gamma_{ij}^2 &= \tilde{\gamma}_{ij}^1 = \frac{1}{\sqrt{2}} [\hat{\tau}_1^K]_{ij}.\end{aligned}$$

The diagonal components in the augmented space coincides with the ones for the regular technique. The non-diagonal ones are found by using the Wick's theorem and noticing that the vertices by themselves do not mix different sectors of the augmented space. The matrix structure displayed by Eq. (27) can be further compactified by equation

$$\hat{\Sigma}_{\alpha\beta} = i\Upsilon_{\alpha\alpha'}^\gamma G_{\alpha'\beta'} \left(\frac{\lambda^2 D_{\gamma\gamma'}}{4} \right) \tilde{\Upsilon}_{\beta'\beta}^{\gamma'}, \quad (29)$$

where $4 \times 4 \times 4$ matrices $\Upsilon_{\alpha\alpha'}^\gamma$ are given by

$$\Upsilon_{(i,j),(i',j')}^{(i'',j'')} = \sum_{\substack{l=0,1 \\ m=0,3}} [\bar{n} (\tau_l^K \otimes \tau_m^a)]_{(i'',j'')} [(\tau_l^K \otimes \tau_m^a)]_{(i,j),(i',j')}, \quad (30a)$$

$$\tilde{\Upsilon}_{(i,j),(i',j')}^{(i'',j'')} = \sum_{\substack{l=0,1 \\ m=0,3}} [(\tau_l^K \otimes \tau_m^a) n]_{(i'',j'')} [(\tau_l^K \otimes \tau_m^a)]_{(i,j),(i',j')}. \quad (30b)$$

Here $\bar{0} \equiv 1$, $\bar{1} = 0$, $\bar{n} = (0, 1; 0, 1)$, $n = (1, 0; 1, 0)^T$, and the sum over index $m = 0, 3$ gives the sum $\tau_0^a \otimes \tau_0^a + \tau_3^a \otimes \tau_3^a$ that is different from zero (and equal 2) only for coinciding indices in the augmented space. Pictorially, this matrix structure can be summarized by Fig. 4 where the basic blocks (boxes and triangles) are again defined in Fig. 2. The appearance of the vector n in the formalism is due to the non-conservation of the number of particles (phonons), see Fig. 2 c).

Note, that the same vertex Υ describes the interaction of the electron with the disorder potential. The only difference is that there is no time dependence

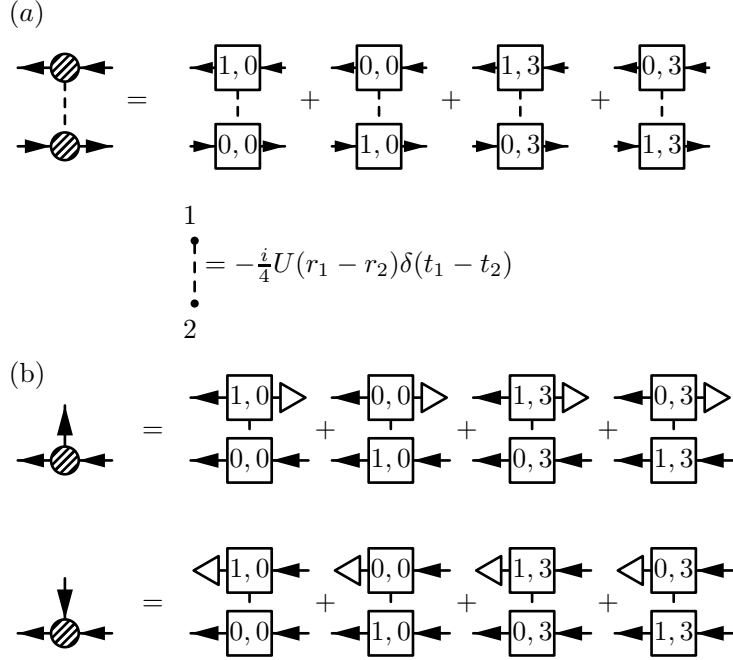


Figure 4: Vertex structure for (a) electron-electron interaction; and (b) for the electron-phonon interaction. The outgoing or ingoing vertical arrow in (b) can be any bosonic line including phonons, photons, impurity potential etc. The short dashed lines on panel (b) are the delta function in space and time.

of the quenched disorder potential, thus the impurity line connecting different branches of the augmented Keldysh contour never decays. The general structure of the vertices for electron-electron interaction is shown in Fig. 4a. Note that it is described by the same building blocks as the electron-phonon and electron-impurity interaction. Because the number of particles in the electron-electron interaction is conserved the vector n does not appear in this case.

The definition of vertices has to be supplied with the remaining bosonic Green functions, defined in Fig. 5

2.8. Diagram technique: summary

We are now prepared to formulate the general rules of the diagram technique that operates with the blocks defined in sections 2.6, 2.7:

In order to compute the correlator (observable or computable) one has: (i) to place the sources and the interaction vertices, (ii) to connect them by the Green function lines, (iii) to trace over the indices in the augmented Keldysh space, (iv) to integrate over positions of the interaction vertices, (v) to multiply the result by $(-1)^{N_L^F}$, where N_L^F is the number of the closed fermionic loops.

As usual, in order to derive the physical properties at large scales one introduces the notion of self-energy that is defined as the sum of all one-particle-

(a)

$$\leftarrow \text{wavy} \rightarrow = \frac{i\lambda^2}{4} \hat{\mathcal{D}}; \quad \leftarrow \text{wavy} \blacktriangleleft = \frac{i\lambda^2}{4} \hat{\mathcal{D}}_0;$$

(b)

$$\blacktriangleleft \dots \blacktriangleleft = V(r_1 - r_2) \hat{\tau}_+^K \otimes [\hat{\tau}_0^a + \hat{\tau}_1^a];$$

Figure 5: Remaining basic elements of the diagram technique for electron-phonon a) and electron-impurity b) interactions. In (a) we include the interaction constant λ into definition of the propagator to keep the vertices of Fig. 4 intact. Correlation function $V(r)$ describes the fluctuations due to the weak random impurities.

irreducible diagrams. For example, the self-energies for the electron-phonon, electron-electron and electron-disorder interaction are shown in Fig. 6.

3. Microscopic Models

The instability expected in section 2.5 is of kinetic nature. Its form depends on the detailed form of the kinetic equation and thus on the microscopic model on which the latter is based. In the following we describe the models that allow one to study the development of the instability in detail.

In all these models the main ingredient are mobile electrons that form a Fermi sea. They are described by the quadratic Hamiltonian

$$H_{el} = \sum_p \xi_p \psi_p^\dagger \psi_p \quad (31)$$

and characterized by the the bare Green function

$$G_0^R = \frac{1}{\epsilon - \xi_p + i0}, \quad G_0^A = \frac{1}{\epsilon - \xi_p - i0}, \quad (32)$$

where the single particle energy ξ_p is counted from the Fermi energy ϵ_F . The condition $\xi_p = 0$ defines the Fermi surface of the electrons.

For electrons the operator H_0 introduced in Eqs. (17) acquires the form

$$H_0 = i\hbar \frac{\partial}{\partial t} - \xi_p, \quad p = -i\hbar \frac{\partial}{\partial r}. \quad (33)$$

Here we restored the units of \hbar for future convenience in developing the quasi-classical approximation later on.

The three models for the electron interaction that we formulate below differ by their conservation laws. The primitive model of electron-phonon interaction (section 3.1) preserves the total energy of the system and the number of electrons but not the momentum of the system. The electrons in the impurity potential (section 3.2) is not a translational invariant system, however, the

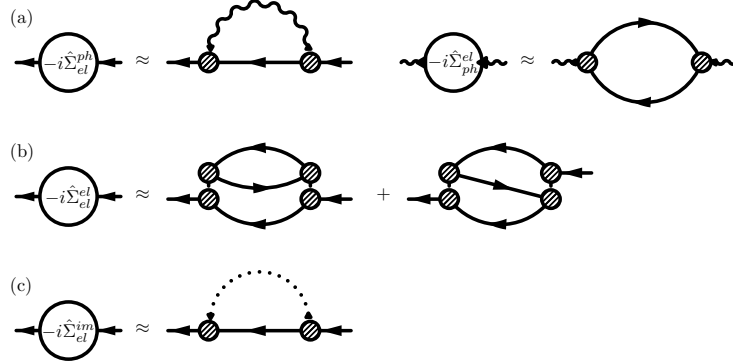


Figure 6: Self-energies for the (a) electron-phonon interaction, (b) electron-electron interaction; and (c) electron in the Gaussian disordered potential. The first order self-energy for the electron electron interaction is discarded as not-related to the collisions but rather renormalizing the self-consistent spectrum for the deterministic motion. The inside lines for the Green function are solid which means that infinite series of the rainbow diagrams is summed. This approximation is known to lead to the quasi-classical Boltzmann equation and can be justified for weak interactions or small enough disorder strength (neglecting localization effects).

scattering by impurities conserves the energy of individual electrons, leading to infinite number of conservation laws in this problem. The electron-electron interaction (section 3.3) preserves both the translational and Galilean invariance, so it conserves the total energy, momentum, and the particle number.⁶

3.1. Electron-phonon interaction

The simplest interacting model is the one in which the electrons interact with dispersionless phonons with frequency ω_0 (Einstein phonons) with Hamiltonian

$$H_{ph} = \sum_r \hbar\omega_0 b_r^\dagger b_r, \quad (34)$$

To avoid inconsequential consideration of the band structure we simply assume (somewhat artificially) that all the points r are random and dilute, their density per unit volume is n_{ph} . Notice that n_{ph} represents the density of phonon sites, the density of thermally excited phonons is the product of n_{ph} and phonon occupation number. Bosons are interacting with electrons via

$$H_{el-ph} = \sum_r u_r \psi^\dagger(r) \psi(r), \quad (35)$$

⁶We neglect the effects of interference of different processes responsible e.g. for the onset of the localization in disordered systems [28] or renormalization of the electron-phonon interaction strength by disorder. The justification for this omission is that the effects considered in this paper are dramatic already on the level of the kinetic equation approximation.

where $u_r = \lambda(b_r + b_r^\dagger)$. Correlators of field u are given by the Green functions local in space,

$$\hbar D_0^R = \frac{2\omega_0 n_{ph} \delta(r_1 - r_2)}{(\omega + i0)^2 - \omega_0^2}, \quad \hbar D_0^A = \frac{2\omega_0 n_{ph} \delta(r_1 - r_2)}{(\omega - i0)^2 - \omega_0^2}. \quad (36)$$

Poles at positive frequencies in these functions correspond to phonon emission and at negative frequencies to phonon absorption (while the physical energies of phonons are of course positive). These Green functions should be used as the basic elements of the diagram technique shown in Fig. 5a. Here and below we adopt the traditional convention in which the phonon frequency is denoted by ω whilst reserving ϵ for the electron energy.

For phonons the operator H_0 , introduced in Eq. 17, acquires the form

$$H_0 = -\frac{\partial^2}{\partial t^2} - \omega_0^2. \quad (37)$$

Similarly to the electrons, see Eq. (20), the Keldysh part of the phonon Green function can be parametrized by

$$D_{\alpha\beta}^K = D_{\alpha}^R \circ \mathcal{P}_{\alpha\beta} - \mathcal{P}_{\alpha\beta} \circ D_{\beta}^A \quad (38)$$

With this parametrization the form of the kinetic equation (21) for the phonons remains the same; the only difference is that their equilibrium distribution functions for the correlated world solution is

$$\hat{\mathcal{P}} = p_{ph}(\omega; r, t) (\hat{\tau}_0^a + \hat{\tau}_1^a) + i\hat{\tau}_2^a, \quad (39)$$

and for the uncorrelated world solution:

$$\hat{\mathcal{P}} = p_{ph}(\omega; r, t) \hat{\tau}_0^a, \quad (40)$$

In the thermal equilibrium $p_{ph} = p_0(\omega)$.

3.2. Electrons in disorder potential

The interaction with quenched disorder potential is described by the Hamiltonian:

$$H_{el-imp} = \sum_r U(r) \psi_r^\dagger \psi_r$$

After averaging over the disorder potential with correlator $\langle U(r)U(r') \rangle = V(r - r')$, the translation invariance is restored for averaged correlation functions and the diagrams for the electron correlators become similar to those for electron-phonon interaction that carries zero frequency, see Fig. 5.

3.3. Electron-electron interaction

The interaction between electrons is given by

$$H_{el-el} = \frac{1}{2} \int \psi_r^\dagger \psi_{r'}^\dagger \psi_{r'} \psi_r U(r-r') dr dr' \quad (41)$$

The rules of the diagram technique are given in Fig. 4. In the discussion of the properties of this model we shall neglect the spin of the electrons. For completeness, we also mention that in the perturbation theory based on Eq. (41) the singular terms proportional to $G^K(t, t)$ have to be understood as $G^K(1, 1) \rightarrow 2i \langle \Psi^\dagger(r_1) \Psi(r_1) \rangle$, and $G^{R,A}(t, t) \rightarrow 0$. Such terms appear only in the Hartree-Fock contributions to the single electron spectrum and not in the collisions interesting for us.

4. Kinetic equation for normal and augmented Keldysh functions.

4.1. Quasiclassical descriptions

The kinetic equation (21) fully determines the evolution of the observables and the computables. However, it is not solvable in a general case. Substantial simplification occurs in the quasiclassical limit in which equations (21) become local in time and phase space. This simplification is possible if the rate of the electron scattering is smaller than the relevant energy scales in the problem: temperature for electron-electron or electron-phonon interactions or Fermi energy for electrons in disorder potential. For the diagonal part of the kinetic equation this is well established and the theory of quantum corrections is well developed, see ref. [29] for a pedestrian introduction. In the following we shall assume that these conditions hold and that the quasiclassical kinetic equation follows for the diagonal terms. Under these conditions similar local equations hold for non diagonal Green functions despite the fact that these functions do not have classical meaning.

We follow the standard procedure for the derivation of the quasiclassical equations for both diagonal and non-diagonal components. Any function of two coordinates and two times can be represented as a Wigner transformation

$$W(t_1, r_1; t_2, r_2) = \int w(\epsilon, p; t, r) e^{i p r_- / \hbar - i \epsilon t_- / \hbar} \frac{d\epsilon d^d p}{(2\pi\hbar)^{d+1}} \quad (42)$$

where $t = (t_1 + t_2)/2$, $r = (r_1 + r_2)/2$, $t_- = t_1 - t_2$, $r_- = r_1 - r_2$. In this section we chose to keep the Planck constant \hbar explicitly so that the parameter for semiclassical expansion is always displayed.

Using this representation for the Green functions of electrons and employing Eq. (33) we get for the left hand side (LHS) of the quantum kinetic equation (21)

$$H_0 \circ \mathcal{F}_{\alpha\beta} - \mathcal{F}_{\alpha\beta} \circ H_0 = i\hbar \left\{ \frac{\partial}{\partial t} + \frac{\partial}{\partial r} \frac{d\xi}{dp} \right\} \mathcal{F}_{\alpha\beta}(\epsilon, p; r, t) \quad (43)$$

which coincides with the LHS of the classical Boltzmann equation for both diagonal and off-diagonal components of the Green functions.

Similar arguments for the phonons lead to the LHS of the kinetic equation

$$H_0 \circ \mathcal{P}_{\alpha\beta} - \mathcal{P}_{\alpha\beta} \circ H_0 = i\hbar\omega \frac{\partial}{\partial t} \mathcal{P}_{\alpha\beta}(\omega, p; r, t). \quad (44)$$

The LHS of Eqs. (43,44) represent the deterministic (Liouville) evolution corresponding to the unitary quantum dynamics which is identical for both diagonal and non-diagonal components in the augmented space. The right hand side (RHS) of the kinetic equation describes the non-reversible probabilistic parts and it is different for different models. The equations

$$\left\{ \frac{\partial}{\partial t} + \frac{\partial}{\partial r} \frac{d\xi}{dp} \right\} \mathcal{F}_{\alpha\beta}(\epsilon, p; r, t) = [\text{St}_{\text{el}}^{\dots}]_{\alpha\beta} \quad (45)$$

$$\omega \frac{\partial}{\partial t} \mathcal{P}_{\alpha\beta}(\omega, p; r, t) = \omega [\text{St}_{\text{ph}}^{\dots}]_{\alpha\beta} \quad (46)$$

describe the time evolution of the distribution functions. Here $[\text{St}_{\text{el}}^{\dots}]$, $[\text{St}_{\text{ph}}^{\dots}]$ denote collision integrals for the particles (electrons or phonons) scattered by other particles (denoted by \dots). These collisions integrals will be computed in the next section.

4.2. Collision integrals for the specific models

The RHS of the kinetic equation allows a number of simplifications in the leading order in \hbar . Furthermore, below we shall consider only the leading order term in the iteration.

In the leading approximation one can replace

$$G^R - G^A = -2\pi i \delta(\epsilon - \xi_p)$$

and, with the same accuracy,

$$G_{\alpha\beta}^K = -2\pi i \delta(\epsilon - \xi_p) \mathcal{F}_{\alpha\beta}.$$

Analogously for phonons

$$\begin{aligned} D^R - D^A &= -2\pi i n_{ph} [\delta(\omega - \omega_0) - \delta(\omega + \omega_0)] \\ D_{\alpha\beta}^K &= -2\pi i [\delta(\omega - \omega_0) \mathcal{P}_{\alpha\beta}(\omega_0) - \delta(\omega + \omega_0) \mathcal{P}_{\alpha\beta}(-\omega_0)]. \end{aligned}$$

Note that the fact that $D_{\alpha\alpha}^K(\omega)$ is an odd function of frequency allows the simultaneous description of phonon emission and absorption processes by a single $\mathcal{P}_{\alpha\alpha}(\omega > 0) > 0$. Substituting these forms into the RHS of the kinetic equation we obtain the collision integrals,

$$\text{St}_{\alpha\beta} = \frac{1}{\hbar} \Im \left\{ [\Sigma_{\alpha}^R \circ \mathcal{F}_{\alpha\beta} - \mathcal{F}_{\alpha\beta} \circ \Sigma_{\beta}^A] - \Sigma_{\alpha\beta}^K \right\}, \quad (47)$$

for different models. In Eq. (47) we kept only the real part of the collision integral, we discuss various approximation involved in its derivation of in more detail in section 4.4

4.2.1. Electron-phonon scattering.

We calculate the lowest order diagrams shown in Fig. 6. For our model one neglect the correlations between phonons at different space locations, i.e. the blobs for fermionic loop in self-energy shown in Fig. 6 a) correspond to coinciding points (with density n_{ph}). This implies that the electron self-energy and collision integral contain an extra factor n_{ph} with respect to the phonon ones. In the diagonal sector we obtain (we do not write down the spatial and time coordinates as the semiclassical collision integrals are local in those variables)

$$\begin{aligned} [\text{St}_{el}^{ph}]_{\alpha\alpha} &= n_{ph} \int \frac{d\omega dP_1 M(P; P_1, \omega)}{(2\pi)(2\pi\hbar)^{(d+1)}} \\ &\quad \times \left\{ - [\mathcal{L}_{el}^{ph}]_{\alpha} (P_1, \omega) \mathcal{F}_{\alpha\alpha}(P) + [\mathcal{P}_{\alpha\alpha}(\omega) \mathcal{F}_{\alpha\alpha}(P_1) + 1] \right\}; \\ [\text{St}_{ph}^{el}]_{\alpha\alpha} &= \frac{1}{2} \int \frac{dP dP_1 M(P; P_1, \omega)}{(2\pi\omega)((2\pi\hbar)^{(d+1)})} \\ &\quad \times \left\{ - [\mathcal{L}_{ph}^{el}]_{\alpha} (P_1, \omega) \mathcal{P}_{\alpha\alpha}(\omega) + [1 - \mathcal{F}_{\alpha\alpha}(P) \mathcal{F}_{\alpha\alpha}(P_1)] \right\}, \end{aligned} \quad (48)$$

where we introduced functions

$$\begin{aligned} [\mathcal{L}_{el}^{ph}]_{\alpha} (P_1, \omega) &= \mathcal{P}_{\alpha\alpha}(\omega) + \mathcal{F}_{\alpha\alpha}(P_1), \\ [\mathcal{L}_{ph}^{el}]_{\alpha} (P_1, \omega) &= \mathcal{F}_{\alpha\alpha}(P) - \mathcal{F}_{\alpha\alpha}(P_1), \end{aligned} \quad (49)$$

that determine outgoing rate. This notation is useful as the same quantity enters the equations for the non-diagonal part.

For off-diagonal ($\alpha \neq \beta$) we obtain

$$\begin{aligned} [\text{St}_{el}^{ph}]_{\alpha\beta} &= n_{ph} \int \frac{dP_1 dQ_1 M(P; P_1, \omega)}{(2\pi)(2\pi\hbar)^{(d+1)}} \left\{ -\mathcal{L}_{el}^{ph}(P_1, \omega) \mathcal{F}_{\alpha\beta}(P) + \mathcal{P}_{\alpha\beta}(\omega) \mathcal{F}_{\alpha\beta}(P_1) \right\}, \\ [\text{St}_{ph}^{el}]_{\alpha\beta} &= \frac{1}{2} \int \frac{dP dP_1 M(Q; P_1, \omega)}{(2\pi\omega)(2\pi\hbar)^{(d+1)}} \left\{ -\mathcal{L}_{ph}^{el}(P_1, \omega) \mathcal{P}_{\alpha\beta}(\omega) - \mathcal{F}_{\alpha\beta}(P) \mathcal{F}_{\beta\alpha}(P_1) \right\}, \end{aligned} \quad (50)$$

where we introduced the short hand notation

$$2\mathcal{L}_{\dots}(P_1, Q_1) \equiv [\mathcal{L}_{\dots}]_u(P_1, Q_1) + [\mathcal{L}_{\dots}]_d(P_1, Q_1). \quad (51)$$

The form factors M include the matrix elements, conservation laws for the electron and phonons colliding with each other, and their spectrum:

$$M = \frac{\lambda^2}{2\hbar} \left[(2\pi\hbar)^{d+1} \delta(\epsilon - \epsilon_1 - \hbar\omega) \right] [2\pi\hbar \delta(\epsilon_1 - \xi(p_1))] \left[2\pi\hbar \sum_{\pm} \pm \delta(\omega \mp \omega_0) \right]$$

where numerical factor 1/2 includes the difference of \mathcal{F}, \mathcal{P} from the physical distribution function by a factor of two. We find it is more convenient to keep

ϵ, ω as independent energies connected by δ -functions in M with physical spectrum to have the symmetric form for the conservation laws and use the $d + 1$ dimensional momentum vector $P = (\epsilon, p)$.

Here comes an important observation. Even though Eq. (48) and Eq. (50) look similar, their properties are very different. Indeed the diagonal part satisfies the electron number conservation law

$$\int dP \left\{ \left[\text{St}_{\text{el}}^{\text{ph}} \right]_{\alpha\alpha} \delta(\epsilon - \xi(p)) \right\} = 0, \quad (52)$$

and the total energy conservation.⁷

$$\int dP \left\{ \left[\text{St}_{\text{el}}^{\text{ph}} \right]_{\alpha\alpha} \delta(\epsilon - \xi(p)) \epsilon \right\} + n_{\text{ph}} \int d\omega \left\{ \left[\text{St}_{\text{ph}}^{\text{el}} \right]_{\alpha\alpha} \hbar\omega \sum_{\pm} \pm \delta(\omega \mp \omega_0) \right\} = 0. \quad (53)$$

Moreover, one can explicitly check that the time derivative of the entropy

$$\begin{aligned} \frac{dS}{dt} = & \int dP \left\{ \left[\text{St}_{\text{el}}^{\text{ph}} \right]_{\alpha\alpha} \delta[\epsilon - \xi(p)] \ln \frac{1 + \mathcal{F}_{\alpha\alpha}(P)}{1 - \mathcal{F}_{\alpha\alpha}(P)} \right\} + \\ & + n_{\text{ph}} \int d\omega \left\{ \left[\text{St}_{\text{ph}}^{\text{el}} \right]_{\alpha\alpha} \sum_{\pm} \pm \delta(\omega \mp \omega_0) \ln \frac{1 + \mathcal{P}_{\alpha\alpha}(\omega)}{\mathcal{P}_{\alpha\alpha}(\omega) - 1} \right\} \geq 0, \quad (54) \end{aligned}$$

which is the microscopic manifestation of Boltzmann H-theorem. Equality is reached only for thermal distribution functions for which it reduces to Eq. (52) and Eq. (53).

These equations allow to prove that the only stable solution of the kinetic equation is given by the thermal distribution functions and all deviations from it decay (generally, exponentially). In contrast, the non-diagonal part does not satisfy any of these properties or conservation laws. As we already mentioned, this absence of conservation laws and H-theorem will be the key to understand the instability of the thermal non-diagonal distributions for correlated worlds (25) and (39) and their subsequent evolution to non-correlated worlds (26), (40). The discussion of the instability will be done in Secs. 5 and 6. In the remainder of this section, we list the properties of the collision integrals for the other physical models of Sec. 3

4.2.2. Electron-electron scattering.

We calculate the lowest order diagram shown on Fig.6. In the diagonal sector we obtain

$$\begin{aligned} \left[\text{St}_{\text{el}}^{\text{el}} \right]_{\alpha\alpha} = & \int \frac{dP_1 dP_2 dP_3 M(P, P_1; P_2 P_3)}{(2\pi\hbar)^{3(d+1)}} \left\{ - \left[\mathcal{L}_{\text{el}}^{\text{el}} \right]_{\alpha} (P_1, P_2, P_3) \mathcal{F}_{\alpha\alpha}(P) \right. \\ & \left. + \left[\mathcal{F}_{\alpha\alpha}(P_3) + \mathcal{F}_{\alpha\alpha}(P_2) - \mathcal{F}_{\alpha\alpha}(P_1) - \mathcal{F}_{\alpha\alpha}(P_1) \mathcal{F}_{\alpha\alpha}(P_2) \mathcal{F}_{\alpha\alpha}(P_3) \right] \right\}, \quad (55) \end{aligned}$$

⁷Note that the momentum is not conserved because of the locality of the phonon correlations even though the averaged system is formally translationally invariant.

where we denoted

$$[\mathcal{L}_{el}^{el}]_{\alpha} = \mathcal{F}_{\alpha\alpha}(P_2)\mathcal{F}_{\alpha\alpha}(P_3) - \mathcal{F}_{\alpha\alpha}(P_1)\mathcal{F}_{\alpha\alpha}(P_3) - \mathcal{F}_{\alpha\alpha}(P_1)\mathcal{F}_{\alpha\alpha}(P_2) + 1. \quad (56)$$

As before, the form factors M include the matrix elements, the conservation laws for the electron and phonons colliding with each other, and their spectrum:

$$M = \frac{|U_{p_2-p} - U_{p_3-p}|^2}{8\hbar} \left[(2\pi\hbar)^{d+1} \delta(P + P_1 - P_2 - P_3) \right] \prod_{i=1}^3 [2\pi\hbar\delta(\epsilon_i - \xi(p_i))]$$

where numerical factor $1/8$ includes the difference of \mathcal{F} , from the physical distribution function by a factor of two, and exchange symmetry of the final state. We find it is more convenient to keep ϵ, ω as independent energies connected by δ -functions in M with physical spectrum to have the symmetric form for the conservation laws and use the $d + 1$ dimensional momentum vectors $P = (\epsilon, p)$.

The collision integral (55) satisfies the conditions similar to those for electron-phonon scattering

$$\int dP \{ [\text{St}_{el}^{el}]_{\alpha\alpha} \delta(\epsilon - \xi(p)) \} = 0, \quad (57)$$

(particle conservation)

$$\int dP \{ [\text{St}_{el}^{el}]_{\alpha\alpha} \delta(\epsilon - \xi(p)) P \} = 0, \quad (58)$$

(electron number conservation)

$$\int dP \left\{ \left[\text{St}_{el}^{\text{ph}} \right]_{\alpha\alpha} \delta(\epsilon - \xi(p)) \ln \frac{1 + \mathcal{F}_{\alpha\alpha}(P)}{1 - \mathcal{F}_{\alpha\alpha}(P)} \right\} \geq 0, \quad (59)$$

(entropy growth).

For off-diagonal ($\alpha \neq \beta$) we obtain

$$[\text{St}_{el}^{el}]_{\alpha\beta} = \int \frac{dP_1 dP_2 dP_3 M(P, P_1; P_2 P_3)}{(2\pi\hbar)^{3(d+1)}} \times \{ -\mathcal{L}_{el}^{el}(P_1, P_2, P_3) \mathcal{F}(P)_{\alpha\beta} + \mathcal{F}_{\alpha\beta}(P_2) \mathcal{F}_{\alpha\beta}(P_3) \mathcal{F}_{\beta\alpha}(P_1) \}, \quad (60)$$

where once again

$$2\mathcal{L}_{el}^{el}(P_1, P_2, P_3) \equiv [\mathcal{L}_{el}^{el}]_u(P_1, P_2, P_3) + [\mathcal{L}_{el}^{el}]_d(P_1, P_2, P_3).$$

Similarly to the electron-phonon interaction, the collision integral (60) for the non-diagonal term is non-linear due to the incoming term. This leads to the instability of the thermal non-diagonal distribution.

4.3. Electron-impurity scattering

The collision integral for the electron-impurity scattering is linear in the distribution function

$$[\text{St}_{\text{el}}^{\text{im}}]_{\alpha\beta} = \int \frac{dp_1 M(p, p_1)}{(2\pi\hbar)^d} \{-\mathcal{F}_{\alpha\beta}(p) + \mathcal{F}_{\alpha\beta}(p_1)\}, \quad (61)$$

where

$$M(p, p_1) = \frac{2\pi}{\hbar} |V_{p-p_1}|^2 \delta(\xi_p - \xi_{p_1}).$$

This implies that in the case of the impurity scattering the non-diagonal components of the Keldysh function have the same time evolution as the diagonal ones, so the solution in which it is equal to the thermal equilibrium distribution is stable. Note that electrons in the impurity potential is a chaotic system. In this respect it is not different from the electron-phonon and the electron-electron interaction. Nevertheless, the non-diagonal components are stable, in contrast to the models with electron-phonon and electron-electron interactions. This results in a very different behavior of the out-of-time-ordered correlators in this system.

4.4. Additional remarks

It is worthwhile to emphasize that the basic form of the kinetic equation and the forthcoming conclusions are not limited to the lowest order self-energy calculation. In particular, taking into account the commutators of the self-energy with $\mathcal{F}_{\alpha\beta}$ results in well controllable corrections to the LHS of the kinetic equation and has the meaning of the self-consistent spectrum. The higher order expansion improves the accuracy of the matrix elements in the collision integrals and also produces the real processes involving larger number of particles. Neither of those complications seem to affect the basic relations of the diagonal and non-diagonal evolutions and we will not be dwelling on them in this paper. The imaginary part of the non-diagonal elements of collision integral neglected in Eq. (47) formally appears due to the difference between the distribution functions in upper and down Worlds:

$$\Im \text{St}_{\alpha\beta} = \frac{1}{\hbar} \Re [\Sigma_{\alpha}^R - \Sigma_{\beta}^R] \mathcal{F}_{\alpha\beta}$$

This effect also disappears in the leading quasiclassical approximation and does not affect the instability discussed in the next sections. For instance, for electron-phonon model this term becomes

$$\Im \text{St}_{\alpha\beta} \propto \int d\xi [\Re D^R(\epsilon - \xi) (\mathcal{F}_{\alpha}(\xi) - \mathcal{F}_{\beta}(\xi)) + \Re G^R(\xi) (\mathcal{P}_{\alpha}(\xi) - \mathcal{P}_{\beta}(\xi))]$$

It disappears for the two Worlds in equilibrium. Furthermore, it is zero if one World has extra particle density that resulted in the spatially non-uniform chemical potential.

5. Instability of the augmented Keldysh functions in zero dimensional case

In this section we study the instability in the systems in which the spatial dependence of the correlation functions can be neglected.

5.1. Instability in electron-phonon model.

The Einstein phonon distribution function is characterized by just two numbers in each sectors of the augmented space that are the values of $\mathcal{P}_{\alpha\beta}(\pm\omega_0)$. In thermal equilibrium the two diagonal components are given by Eq. (39). Because the instability in the non-diagonal sector does not affect the diagonal one (Sec. 2.4), for simplification we assume that the diagonal sector for both electrons and phonons is in equilibrium. This assumption is not essential, and the thermal function can be replaced to its non-equilibrium value without any technical complications. Because the phonon field is real, the non-diagonal sectors are related to each other by the symmetry

$$\mathcal{P}_{ud}(\omega_0) = -\mathcal{P}_{du}(-\omega_0),$$

and the state of the phonons is described by two parameters

$$\begin{aligned}\mathcal{P}_{ud}(\omega_0) &= \theta, \\ \mathcal{P}_{du}(\omega_0) &= \bar{\theta}.\end{aligned}$$

The phonon scattering process does not depend on the electron momentum, so we need to keep only the energy, $\epsilon = \xi(p)$, dependence of the electron distribution function:

$$\begin{aligned}\mathcal{F}_{ud}(\epsilon, p; t) &= f(\epsilon, t), \\ \mathcal{F}_{du}(\epsilon, p; t) &= -\bar{f}(\epsilon, t).\end{aligned}$$

Inserting these definitions in the kinetic equations (45,46,50) and performing integrals over momentum we obtain

$$\tau \frac{\partial f}{\partial t} = -L \left(\frac{\epsilon}{2T}, \frac{\omega_0}{2T} \right) f + [\theta f(\epsilon - \omega_0) + \bar{\theta} f(\epsilon + \omega_0)], \quad (62a)$$

$$\tau \frac{\partial \bar{f}}{\partial t} = -L \left(\frac{\epsilon}{2T}, \frac{\omega_0}{2T} \right) \bar{f} + [\bar{\theta} \bar{f}(\epsilon - \omega_0) + \theta \bar{f}(\epsilon + \omega_0)], \quad (62b)$$

$$\eta\tau \frac{\partial \theta}{\partial t} = -\theta + I_-, \quad (62c)$$

$$\eta\tau \frac{\partial \bar{\theta}}{\partial t} = -\bar{\theta} + I_+, \quad (62d)$$

where we introduced the positive quantities

$$I_{\pm} = \frac{1}{2\omega_0} \int d\epsilon f(\epsilon) \bar{f}(\epsilon \pm \omega_0); \quad (63)$$

$$L(x, y) = 2 \coth(y) - \tanh(x + y) + \tanh(x - y). \quad (64)$$

We also replaced $\hbar\omega_0 \rightarrow \omega_0$ as the semiclassical expansion is already completed. In deriving Eqs. (62), we neglected the energy dependence of the electron density of states, ν , we denoted

$$\frac{1}{\tau} = \frac{2\pi\nu n_{ph}\lambda^2}{\hbar}, \quad (65)$$

and introduced the dimensionless parameter

$$\eta = \frac{n_{ph}}{\hbar\nu\omega_0}. \quad (66)$$

Eqs. (62) are further simplified in the limits $\eta \gg 1$ and $\eta \ll 1$. In the former limit the phonon relaxation is slow compared to electrons, in the latter the electron relaxation is slower. The limit $\eta \ll 1$ seems to be the most relevant for physical situations (e.g. to describe electrons interacting with low density TLS) and moreover it will enable to develop intuition for analyzing the more involved kinetics of electron-electron collisions. Thus we focus on this limit only. Because the relaxation of θ is much faster than that of f , we can solve the Eqs (62c,d) for $\theta, \bar{\theta}$ in the stationary limit. We obtain

$$\tau \frac{\partial f}{\partial t} = -L \left(\frac{\epsilon}{2T}, \frac{\omega_0}{2T} \right) f + [I_- f(\epsilon - \omega_0) + I_+ f(\epsilon + \omega_0)], \quad (67a)$$

$$\tau \frac{\partial \bar{f}}{\partial t} = -L \left(\frac{\epsilon}{2T}, \frac{\omega_0}{2T} \right) \bar{f} + [I_+ \bar{f}(\epsilon - \omega_0) + I_- \bar{f}(\epsilon + \omega_0)]. \quad (67b)$$

Eqs. (67) and Eqs. (63,64) form the complete set of equations describing the time evolution of the non-diagonal components of the distribution function. However, they are still non-linear and nonlocal in energy space.

The further analysis is separated into two regimes: “classical” $\omega_0 \ll T$ and “quantum” $\omega_0 \gg T$. The difference between these regimes is expected on the physical grounds: in the “classical” regime a large number of excitations is already present, therefore, one expects (and we will see that that it is indeed the case) that the perturbation results in the evolution that leads to the uncorrelated fixed point, $f = 0$, $\bar{f} = 0$ with the characteristic time of the order of τ . In the quantum regime, one expects that the characteristic time is determined by an exponentially small number of excitations and it becomes infinite at zero temperature.

Generally, one expects that in the gapful systems at $T = 0$ a small perturbations cannot lead to any instability, in particular, these systems cannot be chaotic, so that the scrambling time is infinite. The exponential growth of the characteristic time at low temperatures in the gapless system found here implies a smooth crossover between the properties of the gapful and gapless systems at $T = 0$.

5.1.1. Classical limit ($\omega_0 \ll T$)

At high temperatures we can neglect ω_0 in I_{\pm} (63) and in the arguments of f in Eq. (67), we can also approximate $L = 2/y$ in Eq. (64). We see then

that the form of $f(\epsilon)$ and $\bar{f}(\epsilon)$ dependencies is not changed by the evolution. Therefore, we can look for the solution of Eq. (67) in the form

$$f(\epsilon) = \phi(t) [1 + \tanh(\epsilon/2T)], \quad (68a)$$

$$\bar{f}(\epsilon) = \phi(t) [1 - \tanh(\epsilon/2T)]. \quad (68b)$$

We obtain that the function $\phi(t)$ obeys the first order differential equation

$$\tau \frac{\partial \phi}{\partial t} = -\frac{4T}{\omega_0} (\phi - \phi^3) \quad (69)$$

that has the unstable fixed point at $\phi = 1$ and the stable fixed point at $\phi = 0$. The solution of this equation takes the form

$$\phi(t) = \left(\frac{1}{1 + \exp[(t - t_d)/t_*^{cl}]} \right)^{1/2}, \quad (70)$$

where $t_*^{cl} = \tau\omega_0/8T$. This time dependence is typical of the dissipative instabilities. The delay time, t_d , depends only logarithmically on the initial conditions: $t_d = t_*^{cl} |\ln[1 - \phi(0)]|$ whilst the decay time t_*^{cl} coincides with the classical scattering time of the electrons that is inversely proportional to the density of phonon sites, n_{ph} , and the phonon occupation number, T/ω_0 . Note that this classical time, t_*^{cl} , is less than the energy relaxation time, in the limit $\omega_0 \ll T$.

5.1.2. Quantum limit ($\omega_0 \gg T$)

In order to describe the behavior of the solution in the quantum limit, it is instructive to look at the results of the numerical solution of Eq. (67) at low temperatures, see Fig. 7. In contrast to the classical case, the function $f(\epsilon)$ does not preserve the shape with the time evolution. However, one observes that the behavior does not change at negative energies. At positive energies we observe a sequence of peaks at energies $\epsilon_n = (n + 1/2)\omega_0$ that are similar to the first peak at $n = 0$. This behavior can be qualitative understood as follows.

At low temperatures Eq. (63) implies that $I_- \gg I_+$ (see also Fig. 7b). If the terms proportional to I_+ are dropped, Eq. (67a) describes the drift of $f(\epsilon)$ to high energies together with relaxation. Similarly, Eq. (67b) describes the drift to negative energies and relaxation. The L -terms in Eqs. (67) lead to decay, so the frequency regime where these terms dominate cannot contribute to the instability. For frequencies $|\epsilon| > \omega_0$ the L -term in Eq. (67) is large so the region responsible for the instability is $|\epsilon| < \omega_0$. In the absence of I_+ , the advection term proportional to I_- removes perturbations from this region. Because the values of $f(\epsilon)$ at high energies does not feedback on low energies, the instability disappears. In order to see the instability it is therefore essential to keep the I_+ term in the region $|\epsilon| < \omega_0$. From Fig. 7b we see that the main contribution to I_{\pm} comes from the vicinity of the frequencies $\pm\omega_0/2$, so the integrals I_{\pm} can be approximated by $I_- \approx f_+^2$ and $I_+ \approx f_-^2$ where $f_{\pm} = f(\pm\omega_0/2)$ (we drop non-essential numerical factors). For this reason we focus on the time dependence of these two values of $f(\epsilon)$. In the equation for df_-/dt we can neglect the

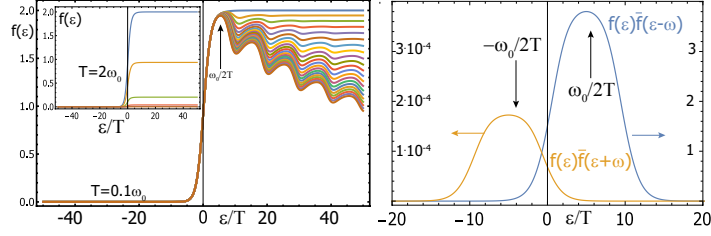


Figure 7: Left panel, main figure: low temperature evolution of non-diagonal parameter f in the low temperature case, $T = 0.1\omega_0$ for discrete times $t/\tau = 0.2, 0.4, \dots, 4.0$. The inset: similar evolution at high temperatures, $T = 2\omega_0$, for $t/\tau = 0.2, 0.4, 0.6, \dots$ shows fast uniform decrease of the non-diagonal parameter. The right panel displays the integrands of I_{\pm} (63) at $t/\tau = 2.0$ that shows that I_{\pm} are dominated by narrow frequency ranges around $\pm\omega_0/2$. This allow us to simplify the equations by considering only the values of f at these points.

contribution of $I_+ f(-3\omega_0/2)$ term because $f(-3\omega_0/2) \sim \exp(-\omega_0/T)f_-$. In the equation for df_-/dt we can neglect the contribution of $I_- f(3\omega_0/2)$ because it is proportional to $I_- \ll 1$. Then the integral equations (67) reduce to two ordinary differential equations:

$$\tau \frac{df_+}{dt} = -L_0 f_+ + f_+^2 f_- \quad (71)$$

$$\tau \frac{df_-}{dt} = -L_0 f_- + f_-^2 f_+ \quad (72)$$

where $L_0 = 2 \exp(-\omega_0/2T)$. At low temperatures the linear term in these equations becomes exponentially small, as a result the instability develops exponentially slowly. Solving for the product $f_+ f_-$ we get

$$f_+ f_- = \frac{L_0}{1 + \exp[(t - t_d)/t_*^{qu}]}, \quad (73a)$$

and

$$f_+ + f_- = f_0 \left(\frac{1}{1 + \exp[(t - t_d)/t_*^{qu}]} \right)^{1/2}, \quad (73b)$$

where $t_*^{qu} = \tau/(2L_0)$. The Eqs. (73) should be compared with the solution (70), we see that they describe similar relaxation but with exponentially smaller rates. Although the behavior of the solution (73) is similar to the one in the high temperature limit, there is an important difference: the relaxation is determined only by a narrow advection region at low energies, whereas the high energy region plays a passive role of a sink. Furthermore, the non-linearity appears first at high energies but it does not affect the fact that the dynamics is determined by the narrow region at low energies that determines the value of I_+ .

5.2. *Instability for electron-electron interaction.*

As for electron-phonon scattering one can focus only on the energy dependence of the off-diagonal functions

$$\mathcal{F}_{ud}(\epsilon, p; t) = f(\epsilon, t), \quad \mathcal{F}_{du}(\epsilon, p; t) = -\bar{f}(\epsilon, t),$$

and assume that the diagonal functions correspond to the equilibrium. As a result, the time evolution of the functions f, \bar{f} is described by the equations similar to Eq. (67):

$$\begin{aligned} \tau_{FL} \frac{\partial f}{\partial t} &= -L_F \left(\frac{\epsilon}{T} \right) f + K(\epsilon, f, \bar{f}), \\ \tau_{FL} \frac{\partial \bar{f}}{\partial t} &= -L_F \left(\frac{\epsilon}{T} \right) \bar{f} + \bar{K}(\epsilon, f, \bar{f}), \\ L_F(x) &= 1 + x^2/\pi^2, \end{aligned} \quad (74)$$

where

$$\tau_{FL}^{-1} \sim T^2/E_F^* \quad (75)$$

is the Fermi liquid relaxation rate, E_F^* is the parameter built from the electron density of states and the interaction constant.⁸ The functional $K(\epsilon, f, \bar{f})$ is of the second order in f and of the first order in \bar{f} :

$$K(\epsilon, f, \bar{f}) = \int_0^\infty I_-(\omega) f(\epsilon - \omega) \frac{d\omega}{2\pi T} + \int_0^\infty I_+(\omega) f(\epsilon + \omega) \frac{d\omega}{2\pi T}, \quad (76a)$$

$$\bar{K}(\epsilon, f, \bar{f}) = \int_0^\infty I_+(\omega) \bar{f}(\epsilon - \omega) \frac{d\omega}{2\pi T} + \int_0^\infty I_-(\omega) \bar{f}(\epsilon + \omega) \frac{d\omega}{2\pi T}, \quad (76b)$$

$$I_\pm(\omega) = 2 \int \frac{d\epsilon}{2\pi T} f(\epsilon) \bar{f}(\epsilon \pm \omega). \quad (76c)$$

Formally these equations are similar to Eqs. (67) for the electron-phonon scattering, the only difference is that instead of one mode Eqs. (76) contain the integral over frequencies. At large $\epsilon \gg T$ the functionals $K(f, \bar{f})$ and $\bar{K}(f, \bar{f})$ are dominated by terms proportional to $I_-(\omega)$ that describes drift to larger frequencies for $f(\epsilon)$ and to smaller frequencies for $\bar{f}(\epsilon)$. The feedback that results in dissipation is due to the energies $\epsilon \lesssim T$. The qualitative properties of these equations are thus captured by the simplified equations for two characteristic values of $f_\pm = f(\pm T)$. These equations have exactly the same form as Eqs. (71,72), with the important difference that $L_0 \sim 1$. Thus their solution is given by the equations (70) with characteristic decay time $t_* \sim \tau_{FL}$.

It is very important that although the relaxation rate in a Fermi liquid becomes very large at high energies, the processes involving high energy electrons

⁸In three dimensional Fermi liquid $E_F^* \sim E_F$ where E_F is the Fermi energy, in two dimensional Fermi liquid it contains additional $\ln(E_F/T)$ factors[30] while in 1D models two particle collisions do not lead to dissipation.

do not contribute to the instability of the equations (74) for the non-diagonal parts. Instead, the instability is controlled by the same processes as the physical relaxation and has characteristic time scale of the electron-electron relaxation time at temperature T .

6. Equations for spatial structure of the instability

As we have seen in section 5 the instability in zero dimensional models is always controlled by equations similar to (62). This equation can be derived and solved analytically in the case of electron-phonon model at high temperatures but it provides the qualitative description in other cases as well. To resolve the spatial structure of the instability we thus begin with the electron-phonon model at high temperatures. The presence of the spacial structure changes the quantum kinetic equations (62) very little (apart from introducing the spacial dependence). Because the phonons in this model are local, the equations for θ and $\bar{\theta}$ contain the fermionic functions taken at the same spatial point. As in section 5.1 in the limit of low phonon density ($\eta \ll 1$) the phonon relaxation is fast, so we can solve for local θ and $\bar{\theta}$:

$$\begin{aligned}\theta(r) &= \frac{1}{2\omega_0} \int d\epsilon f(\epsilon, r) \bar{f}(\epsilon - \omega_0, r), \\ \bar{\theta}(r) &= \frac{1}{2\omega_0} \int d\epsilon f(\epsilon, r) \bar{f}(\epsilon + \omega_0, r),\end{aligned}$$

Performing the standard spatial gradient expansion in the LHS of the kinetic equation (45), we find that df/dt in (62) acquires an additional diffusion term. Parametrizing the solution by the ansatz (68) we obtain the final equation

$$\frac{\partial \phi}{\partial t} - D_* \nabla^2 \phi = -\frac{2(\phi - \phi^3)}{t_*}. \quad (77)$$

This equation is the central result of this paper. As we argue below it holds (with small modifications) for other models as well.

At non-zero temperature the electron-phonon interaction leads to the diffusive motion of electrons characterized by the momentum relaxation time so that the diffusion coefficient $D_* = v_F^2 \tau_{tr} / d$, where v_F is the Fermi velocity and d is the spatial dimensionality. At high temperatures $\omega_0 \ll T$ the transport relaxation rate is given by $1/\tau_{tr} = \lambda^2 \nu (n_{ph} T / \hbar \omega_0)$, with $(n_{ph} T / \hbar \omega_0)_{ph}$ having the meaning of the thermal phonon density. In this case the energy relaxation of the electrons becomes parametrically slower than its momentum relaxation: $1/\tau_e = (\omega_0/T) \lambda^2 \nu n_{ph}$.

The diffusion approximation used to derive Eq. (77) can be rigorously justified only if the resulting gradient of ϕ is small on the scale of the mean free path, $v_F \tau_{tr}$. This happens only if $t_*^{cl} \gg \tau_{tr}$ which can occur if the electron diffusion is additionally slowed down by the impurity scattering $1/\tau_{tr} = 1/\tau_{tr}^{(ph)} + 1/\tau_{tr}^{(imp)} \gg 1/\tau_{tr}^{(ph)}$.

Both the diffusion coefficient D_* and the time t_*^{cl} depend on the local temperature $T(r, t)$ and the electron density $n(r, t)$. Those quantities are described by the standard diffusion and thermal diffusion equations for the diagonal components and their solutions has to be used as entry parameters for Eq. (77). This scheme gives the complete description of the quantum butterfly effect. Notice that depending on the particular model, D_* may coincide with the particle or thermal diffusion coefficients or may be different from those by a numerical factor.

A very similar equation can be put forward for the model of the electron-electron interaction. Taking into account that the effective equations for electron-electron interaction is formally the same as that for electron-phonon case, we write

$$\left(\frac{\partial}{\partial t} + v\nabla\right)\phi - D_*\nabla^2\phi = -\frac{2(\phi - \phi^3)}{t_*}. \quad (78)$$

The only modification here is the appearance of the drift term $v\nabla$ which is dictated by the Galilean invariance for $\xi_p = p^2/2m - \epsilon_F$. The macroscopic velocity $v(r, t)$, the local temperature $T(r, t)$, and the electron density $n(r, t)$ are controlled by the usual equations of local hydrodynamics and thermal (entropy) diffusion [31]. It is possible to generalize Eq. (78) for the case of relativistic hydrodynamics. Based on Lorentz invariance one obtains

$$(u^i\partial_i + D_*\partial_i\partial^i)\phi = -\frac{2(\phi - \phi^3)}{t_*}, \quad (79)$$

where covariant and contravariant component are related by the arbitrary metric tensor and u^i is standard four component velocity vector with local constrain $u_i u^i = 1$.

To close the section, let us emphasize that the coefficients D_*, t_* do not affect the diagonal entropy production and do not enter the usual Onsager relations. It is unknown to us whether there is an analogue of the H -theorem that includes the non-diagonal distribution functions as well.

7. Spatial Propagation of the instability: combustion waves.

The equations (77,78,79) for the spatial structure of the instability are well known in the theory of combustion. In particular, Eq. (77) is very similar to Fisher- Kolmogorov–Petrovsky–Piscounov equation (FKPP) [32, 33]

$$\frac{dy}{dt} - \nabla^2 y = y(1 - y).$$

All equations of this type possess two stationary solutions $y = 0$ and $y = 1$ in case of FKPP, one of them is stable, another is not. In particular, our Eq. (77), displays the instability of the solution $\phi(r) = 1$ that evolves according to the following scenario. After being seeded at time $t = 0$ with the small deviation $\delta\phi(r) = 1 - \phi(r) \ll 1$, in a region around 0 (i.e. $\delta\phi = 0$ for $r > R_c$)

the instability remains localized in the area where it was seeded ($r < R_c$) for the time $t_d \sim \ln(1/\delta\phi)$. After this initial period, the instability starts to grow spatially forming a non-linear wave that moves with a well defined velocity v_{cw} .

For Eq. (77) in 1D the solution $\phi_f(x - v_{cw}t)$ for the front moving with constant velocity v obeys the equation

$$t_* \left(v_{cw} \frac{d\phi_f}{dx} + D_* \frac{d^2\phi_f}{dx^2} \right) = 2\phi_f(1 - \phi_f^2) \quad (80)$$

As is established in the theory of combustion [34], the value of the front velocity can be found from the study of the solution of Eq.(80) at $x \rightarrow \infty$ where $\delta\phi \rightarrow 0$. At $\delta\phi \ll 1$ the solution of Eq. (80) behaves as $\delta\phi \sim \exp(-kx)$ with k that is real at

$$v_{cw}^2 \geq 16D_*/t_*. \quad (81)$$

For the initial conditions that correspond to $\delta\phi = 0$ for $r > R_c$ the solution quickly converges to the one moving with the minimal velocity allowed by the constraint (81). The presence of other solutions (with higher velocities) is due to the fact that for the (non-physical) initial conditions that differ from unity everywhere, the instability develops at large r might develop independently of the seed at small r . One concludes that the combustion wave moves with velocity

$$v_{cw} = 4\sqrt{D_*/t_*}$$

Note that for electron-phonon and electron-electron models $D_* \sim t_* v_F^2$ in the absence of electron-impurity and elastic scattering, so that the front velocity $v_{cw} \sim v_F$. Because no perturbation (even unphysical one) can propagate with velocity larger than v_F , $v_{cw} \lesssim v_F$.

In order to check the conclusions of the semi-quantitative analysis presented above we have studied numerically the front propagation in the dimensionless equation

$$\frac{d\phi}{dt} = \nabla^2\phi + 2\phi(\phi^2 - 1) \quad (82)$$

and in the similar equation describing evolution of both electrons and phonons

$$\frac{d\phi}{dt} = \nabla^2\phi + 2(\Theta - 1)\phi, \quad (83a)$$

$$\frac{d\Theta}{dt} = \phi^2 - \Theta \quad (83b)$$

that describes the situation in which the phonon dynamics is of the same order as electron one (i.e. $\eta = 1$). We found that in all cases and in all dimensions ($d = 1, 2, 3$) the front quickly assumes a well defined shape and start to move with the constant velocity. We note that this conclusion for the two component (electron and phonon) systems is not obvious because such equations are known to display more complex behavior in some cases.

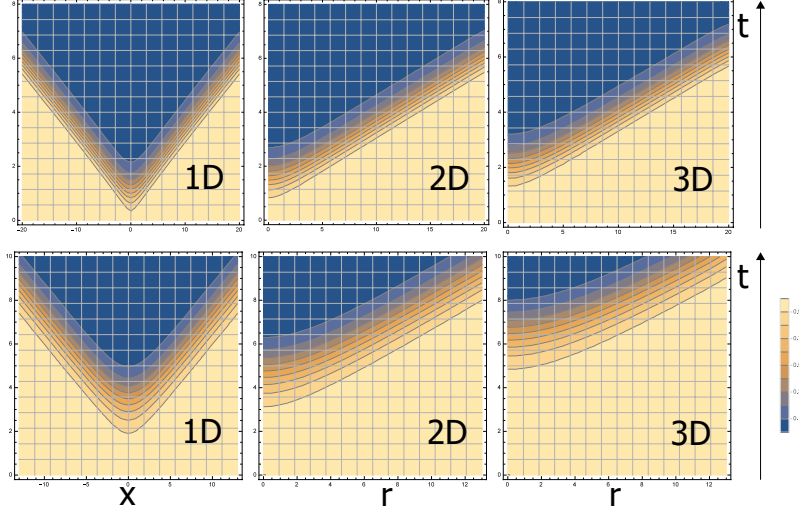


Figure 8: Propagation of instability in different dimensions. The upper panel shows the solution of (82) for one component electron system, the lower for the combined system of electron and phonons (83).

8. Time and spatial dependence of out-of-time-ordered correlators.

We now apply the findings of the previous sections, namely, the instability of the off-diagonal part of the Green function to the computation of the out-of-time-ordered correlator (14). In the conventional theory the correlator of two operators at large separations in time or space factorizes

$$\langle \hat{\mathcal{S}}_0 \hat{\mathcal{R}}_{t,t'} \rangle = \langle \hat{\mathcal{S}}_0 \rangle \langle \hat{\mathcal{R}}_{t,t'} \rangle \quad (84)$$

The corrections to this factorization are given by irreducible correlator that decreases quickly with distance and time. In the electron models considered here the irreducible part is small in $1/p_F r$ and $1/\epsilon_F t$. Furthermore, in a conventional theory one can evaluate both averages in the RHS of (84) against the background of the unperturbed states.

The crucial difference of the two Worlds theory is that the second term in this factorization is unstable. Thus, it is not correct to replace it by its value for the fully correlated, unperturbed state: a small deviation from this value at short distances grows quickly and eventually reduces it to zero in the whole system. Instead one should use for it the results of the solution of the equations for the Green functions discussed in previous sections. In particular, for the response operator in correlator (14) we get

$$\langle \hat{\mathcal{R}}_{t,t'}(r) \rangle = 2\pi\nu [f(\epsilon, t, r) - \bar{f}(\epsilon, t, r)]. \quad (85)$$

where we emphasized that the augmented distribution functions f and \bar{f} are generally the functions of the position in the space as well. The space-time dependence of these functions is determined by the equations derived in Sections 5-7.

The average of the source operator is a constant factor, for the correlator (14) it is given by the total density of electrons:

$$\langle \hat{\mathcal{S}}_0 \rangle = n_{el}. \quad (86)$$

As discussed in Section 5 the time dependence of the augmented distribution functions is simplified in the high temperature regime of the electron-phonon model. In this case the form of the energy dependence of the augmented distribution function does not change with time, the time dependence shows up only in the factor $\phi(r, t)$: $f(\epsilon, t, r) = \phi(r, t)f_0(\epsilon)$. In this case we can write the final result for the Wigner transform of the out-of-time ordered correlator in the closed form

$$\tilde{\mathcal{A}}_{\rho\rho}(\epsilon, t, r) = 2\pi\nu n_0(\epsilon)n_{el}\phi(t, r), \quad (87)$$

$$\mathcal{A}_{\rho\rho}(t', t, r) = \int (d\epsilon) e^{-i\epsilon(t'-t)} \tilde{\mathcal{A}}_{\rho\rho}(\epsilon, \frac{t+t'}{2}, r), \quad (88)$$

Here $\phi(t, r)$ is the solution of the equations (77-79) appropriate for a particular model with the initial conditions

$$\phi(0, r) = 1 - \delta\phi(r) \quad (89)$$

Here

$$\delta\phi(r) \simeq \tilde{\delta}(r)/n_{el} \simeq \tilde{\delta}(r)p_F^{-d} \quad (90)$$

describes the perturbation resulting from the introduction of one extra electron in down World, which serves as a seed of the instability. Here $\tilde{\delta}(r)$ denotes the smeared δ -function that appears because the equations for the distribution function are valid only at the time scales larger than collision time τ_{tr} , so the addition of one particle at time $t = 0$ in the down World translates in the density spread over distance $l_{tr} \sim v_F\tau_{tr}$ for the initial conditions of the Eqs. (77-79). As a result the δ -function in Eq. (90) has to be replaced by $\tilde{\delta}(r)$ which is smeared at the distances of mean free path, $l_{tr} \sim v_F\tau_{tr}$.

The solutions of the equations (77-79) correspond to the propagation of the front as illustrated by Fig. 8.

Note that the particular symmetric form (16) of the response operator computed here has the property that it vanishes at coinciding times and coordinates. This property disappears for less symmetric form of the correlators, for instance if τ_1^a is replaced by, e.g. $\tau_- = \frac{1}{2}(\tau_1 - i\tau_2)$, in the definition of the response operator (16).

$$\tilde{\mathcal{A}}'_{\rho\rho}(t, r) = \left\langle T_C (\bar{\Psi}(t', r)(\tau_1^K \otimes \tau_-^a)\Psi(t, r)) \hat{\mathcal{S}}_0 \right\rangle \quad (91)$$

In this case the first term in (85) disappears and we get after integration over energies

$$\tilde{\mathcal{A}}'_{\rho\rho}(t, r) = 2n_{el}^2 \phi(t, r). \quad (92)$$

At low temperatures for electron-phonon model and for electron-electron interaction at any temperature the energy dependence of the augmented distribution function changes with time as well (Sections 5.1.2, 3.3). In this case the equations for the augmented distribution function are more complicated but the solution remains qualitatively similar.

In all cases, the augmented distribution function that controls the spacial and time dependence of the out-of-time-ordered correlator describes the front propagation, the state of the system before the front has not been affected yet by perturbation whilst the state of the system behind the front is characterized by exponentially vanishing correlations:

$$\tilde{\mathcal{A}}_{\rho\rho}(\epsilon, t, r) = 2\pi\nu n_0(\epsilon) n_{el} \begin{cases} \exp\left(-\frac{t-t_d-r/v_{cw}}{2t_*}\right) & t > r/v_{cw} + t_d \\ 1 - \exp\left(\frac{t-t_d-r/v_{cw}}{t_*}\right) & t < r/v_{cw} + t_d \end{cases} \quad (93)$$

The delay time t_d in these equations is controlled by the initial conditions (89) to the Eqs. (77-79) or similar. It depends only logarithmically on the strength of the initial perturbation:

$$t_d = t_* |\ln[\delta\phi(0)]| \quad (94)$$

Equation (90) enables us to estimate the strength of the initial perturbation. Indeed, $\delta(0) \simeq 1/(v_F \tau_{tr})^d$. Thus, we estimate $\delta\phi(0) \simeq 1/(p_F l_{tr})^d$ and the delay time

$$t_d = t_* d \ln(p_F v_F \tau_{tr}) \quad (95)$$

It is worthwhile to notice that this expression is somewhat similar to the Ehrenfest time [11, 35] appearing as the delay time for the quantum correction in quantum chaos for non-interacting system. In this one electron problem the real instability does not occur.

In a finite size system of spatial size R the correlator (93) decreases exponentially to zero for all $r < R$ after $t_{scr} = t_d + R/v_{cw}$. The time t_{scr} has the meaning of the time at which the two worlds become completely uncorrelated due to a local perturbation, this is also the time that it takes for the quantum information to be spread over the whole system (scrambling time). We see that although the propagation of the information is controlled by diffusion, it occurs with a constant velocity due to the non-linearity of the equations. The diffusion coefficient controls the velocity of this propagation.

The propagation with constant velocity (87,93) also indicates that in a chaotic many body system the entanglement entropy spreads ballistically despite the diffusive nature of the dynamics. This analytical result confirms the empirical conclusions reached in a number of numerical works.

As we discussed above, the conclusions of the linear propagation of the quantum butterfly effect controlled by the combustion equations is quite general. The

details of the equations are sensitive to the microscopic model but the linear propagation similar to combustion front occurs in all of them.

9. Discussion and conclusions

We developed the technique to study the out-of-time-ordered correlators, such as Eq. (1), based on the extension of Keldysh technique. Similarly to standard Keldysh technique, the augmented technique enables the analytical study of systems in different limits, in particular to obtain the leading result in the quasiclassical approximation and systematic corrections to it. As well as in the Keldysh technique the quasiclassical approximation is valid provided that the particle motion between collisions is quasiclassical whilst collision themselves can be quantum.

We limited ourselves to the leading quasiclassical terms that result in the equations similar to the kinetic equation in traditional statistical mechanics. We found that they describe all (or most of all) non-trivial behavior of the out-of-time-ordered correlators. The major difference from the traditional kinetic equation is the appearance of the off-diagonal functions, superficially similar to the conventional distribution function. However, unlike the state occupation probabilities, these new functions also describe the overlap between two copies of the system. The kinetic equation for the off-diagonal functions is dramatically different from that for the diagonal functions: the outgoing term depends on both diagonal and off-diagonal functions whilst the incoming term contains only off-diagonal ones.

The solution with initially unit overlap between two copies becomes unstable when disturbed by a very small perturbation, the phenomenon known as quantum butterfly effect. This instability is described at long times (longer than collision times) by non-linear diffusion equations similar to those appearing in the combustion front propagation. After an initial transient behavior the front of the propagating wave acquires a constant velocity and a shape that does not depend on the initial conditions (Section 7). In the electron models studied in this paper, the velocity of the front is of the order (but less than) the Fermi velocity that serves as natural bound for the propagation speed. In the presence of impurity scattering the velocity of the front can become parametrically slower than Fermi velocity. The microscopic model of electrons interacting with the dilute set of oscillators solved in this work might provide the description of the loss of coherence in the set of two level systems (TLS) that provide both elastic and non-elastic scattering for electrons with the latter becoming small at low temperatures.

Our work suggests a number of exciting developments. First, the quantum butterfly effect studied here can be viewed as the result of the gradual entanglement of the local degrees of freedom with larger and larger part of the surrounding system, and thus is likely to be related to the propagation of entanglement entropy discussed extensively recently [36, 37, 38, 39, 7]. Our results would enable us to put these works on the firm ground of an analytical theory

if the relation between non-diagonal correlators and entanglement entropy is established. We hope to return to this point in future works.

The quantum butterfly effect can be studied numerically and compared with the analytical theory developed here. Also, the destruction of the coherence between two copies of the system might be a useful tool to study the appearance of the arrow of time in the systems described by the unitary evolution. Finally, the destruction of quantum coherence between two copies of the system is a very important phenomenon for the quantum information protocols that are based on the construction of the initially perfectly entangled states of two (or more) interacting qubit systems because small perturbation to one of these systems would result in a spreading decoherence wave described by our equations.

The spatial and time scales of the effective non-linear diffusive equations that describe the instability of the coherent solution are sensitive to the details of the microscopic theory. Furthermore, their relation to the ones appearing in physical observables is not expected to be universal. Thus they might provide a new tool and the new way of thinking about microscopically different systems that display similar properties such as conductivity.

Our formalism can be extended to the study of many body localization by augmenting the formalism developed in the work [40]. This would provide the analytical approach and qualitative understanding to the problem for which only numerical results are currently available.[41, 42, 43, 44] It might even help to describe the transition itself and even the entanglement propagation in generic glassy systems. Moreover, the question of the propagation of the decoherence front in localized systems is similar to the problem of the decoherence propagation in integrable systems. Note that according to [40, 45] in localized and integrable systems the collision integral disappears resulting in the suppression of the chaotic behavior that is responsible for the quantum butterfly effect.

Finally, the microscopic systems studied in this work are described by the combustion equations that display only laminar solution. However, combustion equations for systems with a few components are known to display a large variety of interesting behaviors: Turing instabilities [46], Zhabotinsky cycles [47] to name just a few. It remains to be seen if these solutions are realized in microscopic models as the instabilities of the correlated worlds solution. In particular, they might appear as the solutions against the background of non-equilibrium states such as turbulent hydrodynamics of normal or superfluid liquid.

10. Acknowledgement

We acknowledge extremely useful discussions with Alexei Kitaev and the hospitality of CTP CSIBS, Daejeon, Korea. Our research was supported by ARO grant W911NF-13-1-0431 and by the Russian Science Foundation grant # 14-42-00044.

References

- [1] R. Bradbury, *A sound of thunder and other stories*, William Morrow Paperbacks, New York, Reprint edition (2005).
- [2] A. Larkin, Y. N. Ovchinnikov, Quasiclassical method in the theory of superconductivity, *JETP* 28 (1969) 960.
- [3] A. Kitaev, Hidden Correlations in the Hawking Radiation and Thermal Noise, talk given at Fundamental Physics Prize Symposium, Nov. 10, 2014. Stanford SITP seminars, Nov. 11 and Dec. 18, 2014.
- [4] A. Kitaev, A simple model of quantum holography, KITP strings seminar and Entanglement 2015 program (Feb. 12, April 7, and May 27, 2015).
- [5] J. Maldacena, S. H. Shenker, D. Stanford, A bound on chaos [arXiv:1503.01409](#).
- [6] S. H. Shenker, D. Stanford, Black holes and the butterfly effects, *JHEP* 2014 (2014) 1.
- [7] D. A. Roberts, D. Stanford, L. Susskind, Localized shocks, *JHEP* 2015 (2015) 1.
- [8] B. Swingle, D. Chowdhury, Slow scrambling in disordered quantum systems, [arXiv:1608.03280](#).
- [9] A. Goussev, R. A. Jalabert, P. H. M., W. D. A., Loschmidt echo and time reversal in complex systems, *Phil. Trans. Roy. Soc. A*.
- [10] A. Peres, Stability of quantum motion in chaotic and regular systems, *Phys. Rev. A* 30 (1984) 1610–1615. doi:10.1103/PhysRevA.30.1610. URL <http://link.aps.org/doi/10.1103/PhysRevA.30.1610>
- [11] I. L. Aleiner, A. I. Larkin, Divergence of classical trajectories and weak localization, *Phys. Rev. B* 54 (1996) 14423–14444. doi:10.1103/PhysRevB.54.14423. URL <http://link.aps.org/doi/10.1103/PhysRevB.54.14423>
- [12] O. Agam, I. Aleiner, A. Larkin, Shot noise in chaotic systems: “classical” to quantum crossover, *Phys. Rev. Lett.* 85 (2000) 3153–3156. doi:10.1103/PhysRevLett.85.3153. URL <http://link.aps.org/doi/10.1103/PhysRevLett.85.3153>
- [13] P. Hosur, X.-L. Qi, D. A. Roberts, B. Yoshida, Chaos in quantum channels, *JHEP* 02 (2016) 004. [arXiv:1511.04021](#), doi:10.1007/JHEP02(2016)004.
- [14] Y. Sekino, L. Susskind, Fast scramblers, *Journal of High Energy Physics* 2008 (10) (2008) 065. URL <http://stacks.iop.org/1126-6708/2008/i=10/a=065>

- [15] N. Lashkari, D. Stanford, M. Hastings, T. Osborne, P. Hayden, Towards the Fast Scrambling Conjecture, *JHEP* 04 (2013) 022. [arXiv:1111.6580](#), [doi:10.1007/JHEP04\(2013\)022](#).
- [16] W. Brown, O. Fawzi, Scrambling speed of random quantum circuits [arXiv:1210.6644](#).
- [17] S. H. Shenker, D. Stanford, Multiple Shocks, *JHEP* 12 (2014) 046. [arXiv:1312.3296](#), [doi:10.1007/JHEP12\(2014\)046](#).
- [18] D. Page, Average entropy of a subsystem, *Phys. Rev. Lett.* 71 (1993) 1291.
- [19] B. Swingle, G. Bentsen, M. Schleier-Smith, P. Hayden, Measuring the scrambling of quantum information [arXiv:1602.06271](#).
- [20] N. Y. Yao, F. Grusdt, B. Swingle, M. D. Lukin, D. M. Stamper-Kurn, J. E. Moore, E. A. Demler, Interferometric Approach to Probing Fast Scrambling [arXiv:1607.01801](#).
- [21] D. A. Roberts, B. Swingle, Lieb-robinson bound and the butterfly effect in quantum field theories, *Physical Review Letters* 117 (9) (2016) 091602.
- [22] S. H. Shenker, D. Stanford, Stringy effects in scrambling, *Journal of High Energy Physics* 2015 (5) (2015) 1–34. [doi:10.1007/JHEP05\(2015\)132](#).
URL [http://dx.doi.org/10.1007/JHEP05\(2015\)132](http://dx.doi.org/10.1007/JHEP05(2015)132)
- [23] M. Blake, Universal charge diffusion and the butterfly effect in holographic theories, *Phys. Rev. Lett.* 117 (2016) 091601. [doi:10.1103/PhysRevLett.117.091601](#).
URL <http://link.aps.org/doi/10.1103/PhysRevLett.117.091601>
- [24] L. V. Keldysh, Diagram technique for nonequilibrium processes, *Sov. Phys. JETP* 20 (1965) 1018.
- [25] M. Ansari, Y. V. Nazarov, Keldysh formalism for multiple parallel worlds, *J. Exp. Theor. Phys.* 122 (3) (2016) 389–401. [arXiv:1509.04253](#), [doi:10.1134/S1063776116030134](#).
- [26] A. Larkin, Y. N. Ovchinnikov, Nonlinear conductivity of the superconductors in the mixed state, *JETP* 41 (1975) 1200.
- [27] J. Rammer, *Quantum Field Theory of Non-Equilibrium States*, Cambridge University Press, 2007.
- [28] B. Altshuler, A. Aronov, Fermi-liquid theory of the electron-electron interaction effects in disordered metals, *Solid State Communications* 46 (6) (1983) 429 – 435. [doi:http://dx.doi.org/10.1016/0038-1098\(83\)90570-7](#).
URL <http://www.sciencedirect.com/science/article/pii/0038109883905707>

- [29] A. Kamenev, *Field Theory of Non-Equilibrium Systems*, Cambridge University Press, 2011.
URL <https://books.google.it/books?id=mrH1mAEACAAJ>
- [30] B. N. Narozhny, G. Zala, I. L. Aleiner, Interaction corrections at intermediate temperatures: Dephasing time, *Phys. Rev. B* 65 (2002) 180202. doi:10.1103/PhysRevB.65.180202.
URL <http://link.aps.org/doi/10.1103/PhysRevB.65.180202>
- [31] L. P. Pitaevskii, E. M. Lifshitz, *Physical Kinetics: Volume 10*, Pergamon Press, 1981.
- [32] R. A. Fisher, The wave of advance of advantageous genes, *Annals of Eugenics* 7 (4) (1937) 355–369. doi:10.1111/j.1469-1809.1937.tb02153.x.
URL <http://dx.doi.org/10.1111/j.1469-1809.1937.tb02153.x>
- [33] A. Kolmogorov, I. Petrovsky, N. Piscounov, Study of the diffusion equation with growth of the quantity of matter and its application to a biological problem, *Bull. State Univ. Mosc.* (1937) 1–25.
- [34] Y. B. Zeldovich, G. I. Barenblatt, V. Librovich, G. Makhviladze, *The Mathematical Theory of Combustion and Explosions*, Plenum, 1985.
- [35] I. L. Aleiner, A. I. Larkin, Role of divergence of classical trajectories in quantum chaos, *Phys. Rev. E* 55 (1997) R1243.
- [36] P. Calabrese, J. Cardy, Evolution of entanglement entropy in one-dimensional systems, *Journal of Statistical Mechanics: Theory and Experiment* 2005 (04) (2005) P04010.
URL <http://stacks.iop.org/1742-5468/2005/i=04/a=P04010>
- [37] T. Hartman, J. Maldacena, Time evolution of entanglement entropy from black hole interiors, *JHEP* 05 (2013) 014. doi:10.1007/JHEP05(2013)014.
- [38] H. Casini, H. Liu, M. Mezei, Spread of entanglement and causality, *JHEP* 07 (2016) 077. arXiv:1509.05044, doi:10.1007/JHEP07(2016)077.
- [39] J. H. Bardarson, F. Pollmann, J. E. Moore, Unbounded growth of entanglement in models of many-body localization, *Physical Review Letters* 109 (1) (2012) 17202.
- [40] D. Basko, I. Aleiner, B. Altshuler, Metal insulator transition in a weakly interacting many-electron system with localized single-particle states, *Annals of Physics* 321 (5) (2006) 1126 – 1205. doi:http://dx.doi.org/10.1016/j.aop.2005.11.014.
URL <http://www.sciencedirect.com/science/article/pii/S0003491605002630>
- [41] Y. Chen, Quantum Logarithmic Butterfly in Many Body Localization, ArXiv e-prints arXiv:1608.02765.

- [42] H. Shen, P. Zhang, R. Fan, H. Zhai, Out-of-Time-Order Correlation at a Quantum Phase Transition, ArXiv e-prints [arXiv:1608.02438](https://arxiv.org/abs/1608.02438).
- [43] R. Fan, P. Zhang, H. Shen, H. Zhai, Out-of-Time-Order Correlation for Many-Body Localization, ArXiv e-prints [arXiv:1608.01914](https://arxiv.org/abs/1608.01914).
- [44] Y. Huang, Y.-L. Zhang, X. Chen, Out-of-Time-Ordered Correlator in Many-Body Localized Systems, ArXiv e-prints [arXiv:1608.01091](https://arxiv.org/abs/1608.01091).
- [45] A. M. Lunde, K. Flensberg, L. I. Glazman, Three-particle collisions in quantum wires: Corrections to thermopower and conductance, Phys. Rev. B 75 (2007) 245418. doi:10.1103/PhysRevB.75.245418.
URL <http://link.aps.org/doi/10.1103/PhysRevB.75.245418>
- [46] A. Turing, The chemical basis of morphogenesis, Phil. Trans. Roy. Soc. B 237 (1952) 37–72.
- [47] A. M. Zhabotinsky, Periodic oxidation of malonic acid in solution (a study of the belousov reaction kinetics), Biofizika 9 (1964) 306–311.